

1 **Holocene aridification trend and human impact interrupted by millennial- and centennial-**
2 **scale climate fluctuations from a new sedimentary record from Padul (Sierra Nevada,**
3 **southern Iberian Peninsula)**

4 María J. Ramos-Román¹, Gonzalo Jiménez-Moreno¹, Jon Camuera¹, Antonio García-Alix¹, R.
5 Scott Anderson², Francisco J. Jiménez-Espejo³, José S. Carrión⁴

6 ¹ Departamento de Estratigrafía y Paleontología, Universidad de Granada, Spain

7 ² School of Earth Sciences and Environmental Sustainability, Northern Arizona University,
8 USA.

9 ³ Department of Biogeochemistry, Japan Agency for Marine-Earth Science and Technology
10 (JAMSTEC), Japan.

11 ⁴ Departamento de Biología Vegetal, Facultad de Biología, Universidad de Murcia, Murcia,
12 Spain.

13 *Correspondence to:* María J. Ramos-Román (mjrr@ugr.es)

14 **Abstract.** Holocene centennial-scale paleoenvironmental variability has been described in a
15 multiproxy analysis (i.e. lithology, geochemistry, macrofossil and microfossil analyses) of a
16 paleoecological record from the Padul basin in Sierra Nevada, southern Iberian Peninsula. This
17 sequence covers a relevant time interval hitherto unreported in the studies of the Padul
18 sedimentary sequence. The ~4700 yr-long record has preserved proxies of climate variability,
19 with vegetation, lake levels and sedimentological change during the Holocene in one of the most
20 unique and southernmost peat bogs from Europe. The progressive Middle and Late Holocene
21 trend toward arid conditions identified by numerous authors in the western Mediterranean
22 region, mostly related to a decrease in summer insolation, is also documented in this record,
23 being here also superimposed by centennial-scale variability in humidity. In turn, this record
24 shows centennial-scale climate oscillations in temperature that correlate with well-known
25 climatic events during the Late Holocene in the western Mediterranean region, synchronous with
26 variability in solar and atmospheric dynamics. The multiproxy Padul record first shows a
27 transition from a relatively humid Middle Holocene in the western Mediterranean region to more
28 aridity from ~4700 to ~2800 cal yr BP. A relatively warm and humid period occurred between
29 ~2600 to ~1600 cal yr BP, coinciding with persistent negative NAO conditions and the historic
30 Iberian-Roman Humid Period. Enhanced arid conditions, co-occurring with overall positive
31 NAO conditions and increasing solar activity, are observed between ~1550 to ~450 cal yr BP
32 (~400 to ~1400 CE) and colder and warmer conditions happened during the Dark Ages and
33 Medieval Climate Anomaly, respectively. Slightly wetter conditions took place during the end of
34 the MCA and the first part of the Little Ice Age, which could be related to a change towards
35 negative NAO conditions and minima in solar activity. Time series analysis performed from
36 local (*Botryococcus* and TOC) and regional (Mediterranean forest) signals helped us determining
37 the relationship between southern Iberian climate evolution, atmospheric, oceanic dynamics and
38 solar activity. Our multiproxy record shows little evidence of human impact in the area until
39 ~1550 cal yr BP, when evidence of agriculture and livestock grazing occurs. Therefore climate is
40 the main forcing mechanism controlling environmental change in the area until relatively
41 recently.

42

43 **Keywords:** Holocene, Padul, peat bog, North Atlantic Oscillation, atmospheric dynamics,
44 southern Iberian Peninsula, Sierra Nevada, western Mediterranean.

45 **1 Introduction**

46 The Mediterranean area is situated in a sensitive region between temperate and subtropical
47 climates making it an important place to study the connections between atmospheric and oceanic
48 dynamics and environmental change. Climate in the western Mediterranean and the southern
49 Iberian Peninsula is influenced by several atmospheric and oceanic dynamics (Alpert et al.,
50 2006), including the North Atlantic Oscillation (NAO) one of the principal atmospheric
51 phenomenon controlling climate in the area (Hurrell, 1995; Moreno et al., 2005). Recent NAO
52 reconstructions in the western Mediterranean relate negative and positive NAO conditions with
53 an increase and decrease, respectively, in winter (effective) precipitation (Olsen et al., 2012;
54 Trouet et al., 2009). Numerous paleoenvironmental studies in the western Mediterranean have
55 detected a link at millennial- and centennial-scales between the oscillations of paleoclimate
56 proxies from sedimentary records with solar variability and atmospheric (i.e., NAO) and/or
57 ocean dynamics during the Holocene (Fletcher et al., 2013; Moreno et al., 2012; Rodrigo-Gámiz
58 et al., 2014). Very few montane and low altitude lake records in southern Iberia document
59 centennial-scale climate change [see, for example Zoñar Lake (Martín-Puertas et al., 2008)], with
60 most terrestrial records in the western Mediterranean region evidencing only millennial-scale
61 cyclical changes. Therefore, higher-resolution decadal-scale analyses are necessary to analyze
62 the link between solar activity, atmospheric and oceanographic systems with terrestrial
63 environment in this area at shorter (i.e., centennial) time scales.

64
65 Sediments from lakes, peat bogs and marine records from the western Mediterranean have
66 documented an aridification trend during the Late Holocene (Carrión et al., 2010; Gil-Romera et
67 al., 2010; Jalut et al., 2009). This trend, however, was superimposed by shorter-term climate
68 variability, as shown by several recent studies from the region (Carrión, 2002; Fletcher et al.,
69 2013; Jiménez-Moreno et al., 2013; Martín-Puertas et al., 2008; Ramos-Román et al., 2016).
70 This relationship between climate variability, culture evolution and human impact during the
71 Late Holocene has also been the subject of recent paleoenvironmental studies (Carrión et al.,
72 2007; Lillios et al., 2016; López-Sáez et al., 2014; Magny, 2004). However, it is still unclear
73 whether climate or human activities have been the main forcing driving environmental change
74 (i.e., deforestation) in this area during this time.

75
76 Within the western Mediterranean, Sierra Nevada is the highest and southernmost mountain
77 range in the Iberian Peninsula and thus presents a critical area for paleoenvironmental studies.
78 Most high-resolution studies there have come from high elevation sites. The well-known Padul
79 peat bog site is located at the western foot of the Sierra Nevada (Fig. 1) and bears one of the
80 longest continental records in southern Europe, with a sedimentary sequence of ~100 m thick
81 that could represent the last 1 Ma (Ortiz et al., 2004). Several research studies, including
82 radiocarbon dating, geochemistry and pollen analyses, have been carried out on previous cores
83 from Padul, and have documented glacial/interglacial cycles during the Pleistocene and up until
84 the Middle Holocene. However, the Late Holocene section of the Padul sedimentary sequence
85 has never been effectively retrieved and studied (Florschütz et al., 1971; Ortiz et al., 2004; Pons
86 and Reille, 1988). This was due to the location of these previous corings within a current peat

87 mine operation, where the upper (and non- productive) part of the sedimentary sequence was
88 missing.

89
90 Here we present a new record from the Padul peat bog basin: Padul-15-05, a 42.64 m-long
91 sediment core that, for the first time, contains a continuous record of the Late Holocene (Fig. 2).
92 A high-resolution multi-proxy analysis of the upper 1.15 m, the past ~4700 cal yr BP, has
93 allowed us to determine a complete paleoenvironmental and paleoclimatic record at centennial-
94 and millennial-scales. To accomplish that, we reconstructed changes in the Padul peat bog
95 vegetation, sedimentation, climate and human impact during the Holocene throughout the
96 interpretation of the lithology, palynology and geochemistry.

97
98 Specifically, the main objective of this paper is to determine environmental variability and
99 climate evolution in the southern Iberian Peninsula and the western Mediterranean region and
100 their linkages to northern hemisphere climate and solar variability during the latter Holocene. In
101 order to do this, we compared our results with other paleoclimate records from the region and
102 solar activity from the northern hemisphere for the past ~4700 cal yr BP (Bond et al., 2001;
103 Laskar et al., 2004; Sicre et al., 2016; Steinhilber et al., 2009).

104 **2 Study site**

105 **2.1 Regional setting: Sierra Nevada climate and vegetation**

106 Sierra Nevada is a W-E aligned mountain range located in Andalucía (southern Spain). Climate
107 in this area is Mediterranean, with cool and humid winters and hot/warm summer drought. In the
108 Sierra Nevada, the mean annual temperature at approximately 2500 m asl is 4.5 °C and the mean
109 annual precipitation is 700 mm/yr (Oliva et al., 2009). Sierra Nevada is strongly influenced by
110 thermal and precipitation variations due to the altitudinal gradient (from ca. 700 to more than
111 3400 m), which control plant taxa distribution in different bioclimatic vegetation belts due to the
112 variability in thermotypes and ombrotypes (Valle Tendero, 2004). According to the
113 climatophilous series classification, Sierra Nevada is divided in four different vegetation belts
114 (Fig. 1). The crioromediterranean vegetation belt, occurring above ~2800 m, is characterized by
115 tundra vegetation and principally composed by species of Poaceae, Asteraceae, Brassicaceae,
116 Gentianaceae, Scrophulariaceae and Plantaginaceae between other herbs, with a number of
117 endemic plants (e.g. *Erigeron frigidus*, *Saxifraga nevadensis*, *Viola crassiuscula*, *Plantago*
118 *nivalis*). The oromediterranean belt, between ~ 1900 to ~2800 m, is principally made up of
119 *Pinus sylvestris*, *P. nigra* and *Juniperus* spp. and other shrubs such as species of Fabaceae,
120 Cistaceae and Brassicaceae. The supramediterranean belt, from ~ 1400 to 1900 m of elevation,
121 bears principally *Quercus pyrenaica*, *Q. faginea* and *Q. rotundifolia* and *Acer opalus* ssp.
122 *granatense* with other trees and shrubs, including members of the Fabaceae, Thymelaeaceae,
123 Cistaceae and *Artemisia* sp. being the most important. The mesomediterranean vegetation belt
124 occurs between ~600 and 1400 m of elevation and is principally characterized by *Quercus*
125 *rotundifolia*, some shrubs, herbs and plants as *Juniperus* sp., and some species of Fabaceae,
126 Cistaceae and Liliaceae with others (Al Aallali et al., 1998; Valle, 2003). The human impact over
127 this area, especially important during the last millennium, affected the natural vegetation
128 distribution through fire, deforestation, cultivation (i.e., *Olea*) and subsequent reforestation
129 (mostly *Pinus*) (Anderson et al., 2011).

130 2.2 Padul peat bog

131 The Padul basin is situated at approximately 725 m elevation in the southeastern part of the
132 Granada Basin, at the foothill of the southwestern Sierra Nevada, Andalucía, Spain (Fig. 1). This
133 is one of the most seismically active areas in the southern Iberian Peninsula with numerous faults
134 in NW-SE direction, with the Padul fault being one of these active normal faults (Alfaro et al.,
135 2001). It is a small extensional basin approximately 12 km long and covering an area of
136 approximately 45 km², which is bounded by the Padul normal fault. The sedimentary in-filling of
137 the basin consists of Neogene and Quaternary deposits; Upper Miocene conglomerates,
138 calcarenites and marls, and Pliocene and Quaternary alluvial sediments, lacustrine and peat bog
139 deposits (Sanz de Galdeano et al., 1998; Delgado et al., 2002; Domingo et al., 1983). Vegetation
140 in the Padul area is dominated by *Q. rotundifolia* (and in less amounts *Q. faginea*), which is
141 normally accompanied by *Pistacia terebinthus*. Shrub species in the area include *Juniperus*
142 *oxycedrus*, *Crataegus monogyna*, *Daphne gnidium* and *Ruscus aculeatus*. Creepers such as
143 *Lonicera implexa*, *Rubia peregrina*, *Hedera helix*, *Asparagus acutifolius* also occur in this area
144 and some herbs, such as *Paeonia broteroi*. *Quercus coccifera* also occurs in ridgecrests and very
145 sunny rocky outcrops. *Retama sphaerocarpa* and *Genista cinerea* subsp. *speciosa* and the
146 *Thymo-Stipetum tenacissime* series also occur in sunny areas and in more xeric soils.
147 Nitrophilous communities occur in soils disrupted by livestock, pathways or open forest,
148 normally related with anthropization (Valle, 2003).

149
150 The Padul peat bog is endorheic, with a surface of approximately 4 km² placed in the Padul basin
151 that contains a sedimentary sequence characterized mostly by peat accumulation. The basin fill is
152 asymmetric, with thicker sedimentary and peat infill to the northeast (~100 m thick; Domingo-
153 García et al., 1983; Florschütz et al., 1971; Nestares and Torres, 1997) and progressively
154 becoming thinner to the southwest (Alfaro et al., 2001). The main source area of allochthonous
155 sediments in the bog is the Sierra Nevada, which is characterized at higher elevations by
156 Paleozoic siliceous metamorphic rocks (mostly mica-schists and quartzites) from the Nevado-
157 Filabride complex and, at lower elevations and acting as bedrock, by Triassic dolomites,
158 limestones and phyllites from the Alpujárride Complex (Sanz de Galdeano et al. 1998).
159 Geochemistry in the Padul sediments is influenced by detritic materials also primarily from from
160 the the Sierra Nevada (Ortiz et al., 2004). Groundwater inputs into the Padul basin come from
161 the Triassic carbonates aquifers (N and S edge to the basin), the out flow of the Granada Basin (W
162 edge to the basin) and the conglomerate aquifer to the east edge (Castillo Martín et al., 1984;
163 Ortiz et al., 2004). The main water output is by evaporation and evapotranspiration, water wells
164 and by canals (“madres”) that drain the water to the Dúrcal river to the southeast (Castillo Martín
165 et al., 1984). Climate in the Padul area is characterized by a mean annual temperature of 14.4 °C
166 and a mean annual precipitation of 445 mm (<http://www.aemet.es/>).

167 The Padul-15-05 drilling site was located ~50 m south of the present-day Padul lake shore area.
168 This basin area is presently subjected to seasonal water level fluctuations and is principally
169 dominated by *Phragmites australis* (Poaceae). The lake environment is dominated by aquatic
170 and wetland communities with *Chara vulgaris*, *Myriophyllum spicatum*, *Potamogeton*
171 *pectinatus*, *Potamogetum coloratus*, *Phragmites australis*, *Typha dominguensis*, *Apium*
172 *nodiflorum*, *Juncus subnodulosus*, *J. bufonius*, *Carex hispida* and *Ranunculus muricatus*, among
173 others (Pérez Raya and López Nieto, 1991). Some sparse riparian trees occur in the northern lake
174 shore, such as *Populus alba*, *Populus nigra*, *Salix* sp., *Ulmus minor* and *Tamarix*. At present

175 *Phragmites australis* is the most abundant plant bordering the lake. Surrounding this area are
176 cultivated crops with cereals, such as *Triticum* spp., as well as *Prunus dulcis* and *Olea europea*.
177

178 **3 Material and methods**

179 Two sediment cores, Padul-13-01 (37°00'40''N; 3°36'13''W) and Padul-15-05 (37°00'39.77''N;
180 3°36'14.06''W) with a length of 58.7 cm and 42.64 m, respectively, were collected between
181 2013 and 2015 from the peat bog (Fig. 1). The cores were taken using a Rolatec RL-48-L drilling
182 machine equipped with a hydraulic piston corer from the Scientific Instrumentation Centre of the
183 University of Granada (UGR). The sediment cores were wrapped in film, put in core boxes,
184 transported to UGR and stored in a dark cool room at 4°C.

185 **3.1 Age-depth model (AMS radiocarbon dating)**

186 The core chronology was constrained using fourteen AMS radiocarbon dates from plant remains
187 and organic bulk samples taken from the cores (Table 1). In addition, one sample with
188 gastropods was also submitted for AMS radiocarbon analysis, although it was rejected due to
189 important reservoir effect, that provided a very old date. Thirteen of these samples came from
190 Padul-15-05 with one from the nearby Padul-13-01 (Table 1). We were able to use this date from
191 Padul-13-01 core as there is a very significant correlation between the upper part of Padul-15-05
192 and Padul-13-01 cores, shown by identical lithological and geochemical changes (Supplementary
193 information 1; Figure S1). The age model for the upper ~3 m minus the upper 21 cm from the
194 surface was built using the R-code package 'Clam 2.2' (Blaauw, 2010) employing the calibration
195 curve IntCal 13 (Reimer et al., 2013), a 95 % of confidence range, a smooth spline (type 4) with
196 a 0.20 smoothing value and 1000 iterations (Fig. 2). The chronology of the uppermost 21 cm of
197 the record was built using a linear interpolation between the last radiocarbon date and the top of
198 the record (Present; 2015 CE). Even though the length of the Padul-15-05 core is ~43 m, the
199 studied interval in the work presented here is the uppermost 115 cm of the record that are
200 constrained by seven AMS radiocarbon dates (Fig. 2).

201 **3.2 Lithology, MS, XRF and TOC**

202 Padul-15-05 core was split longitudinally and was described in the laboratory with respect to
203 lithology and color (Fig. 3). Magnetic susceptibility (MS) was measured with a Bartington MS3
204 operating with a MS2E sensor. MS measurements (in SI units) were obtained directly from the
205 core surface every 0.5 cm (Fig. 3).

206
207 Elemental geochemical composition was measured in an X-Ray fluorescence (XRF) Avaatech
208 core scanner® at the University of Barcelona (Spain). A total of thirty-three chemical elements
209 were measured in the XRF core scanner at 10 mm of spatial resolution, using 10 s count time, 10
210 kV X-ray voltage and a X-ray current of 650 µA for lighter elements and 35 s count time, 30 kV
211 X-ray voltage, X-ray current of 1700 µA for heavier elements. Thirty-three chemical elements
212 were measured but only the most representative with a major number of counts were considered
213 (Si, K, Ca, Ti, Fe, Zr, Br and Sr). Results for each element are expressed as intensities in counts
214 per second (cps) and normalized (norm.) for the total sum in cps in every measure (Fig. 3).

215 Total organic carbon (TOC) was analyzed every 2 or 3 cm throughout the core. Samples were
216 previously decalcified with 1:1 HCl in order to eliminate the carbonate fraction. The percentage
217 of organic Carbon (OC %) was measured in an Elemental Analyzer Thermo Scientific Flash
218 2000 model from the Scientific Instrumentation Centre of the UGR (Spain). Percentage of TOC
219 per gram of sediment was calculated from the percentage of organic carbon (OC %) yielded by
220 the elemental analyzer, and recalculated by the weight of the sample prior to decalcification (Fig.
221 3).

222 3.3 Pollen and NPP

223 Samples for pollen analysis (1-3 cm³) were taken every 1 cm throughout the core, with a total of
224 103 samples analyzes. Pollen extraction methods followed a modified Faegri and Iversen (1989)
225 methodology. Processing included the addition of *Lycopodium* spores for calculation of pollen
226 concentration. Sediment was treated with NaOH, HCl, HF and the residue was sieved at 250 µm
227 previous to an acetolysis solution. Counting was performed using a transmitted light microscope
228 at 400 magnifications to an average pollen count of ca. 260 terrestrial pollen grains. Fossil pollen
229 was identified using published keys (Beug, 2004) and modern reference collections at University
230 of Granada (Spain). Pollen counts were transformed to pollen percentages based on the terrestrial
231 pollen sum, excluding aquatics. The palynological zonation was executed by cluster analysis
232 using twelve primary pollen taxa- *Olea*, *Pinus*, deciduous *Quercus*, evergreen *Quercus*, *Pistacia*,
233 Ericaceae, *Artemisia*, Asteroideae, Cichorioideae, Amaranthaceae and Poaceae (Grimm, 1987)
234 (Fig. 4). Non-pollen palynomorphs (NPP) include fungal and algal spores, and thecamoebians
235 (testate amoebae). The NPP percentages were calculated and represented with respect to the
236 terrestrial pollen sum (Fig. 4). Furthermore, some pollen taxa were grouped, according to
237 present-day ecological bases, into Mediterranean forest and xerophytes (Fig. 4). The
238 Mediterranean forest taxa is composed of *Quercus* total, *Olea*, *Phillyrea* and *Pistacia*. The
239 xerophyte group includes *Artemisia*, *Ephedra*, and Amaranthaceae.

240 4 Results

241 4.1 Chronology and sedimentation rates

242 The age-model of the upper 115 cm of Padul-15-05 core (Fig. 2) shows an average sedimentation
243 rate (SAR) of 0.058 cm/yr over last ~4700 cal yr BP, being the age constrained by seven AMS
244 ¹⁴C dates (Table 1). However, SARs of individual core segments vary from 0.01 to 0.11 cm/yr
245 (Fig. 2).

246 4.2 Lithology, MS, XRF and TOC

247 The stratigraphy of the upper ~115 cm of the Padul-15-05 sediment core was deduced primarily
248 by visual inspection. However, our visual inspections were support by comparison with the
249 element geochemical composition (XRF), the MS of the split cores, and TOC (Fig. 3) to
250 determine shifts in sediment facies. The lithology for this sedimentary sequence consists in clays
251 with variable carbonates, siliciclastics and organic content (Fig. 3). We also used a Linear r
252 (Pearson) correlation to calculated relationship for the XRF data. The correlation for the
253 inorganic geochemical elements determined two different groups of elements that covary (Table
254 2): Group 1) Si, K, Ti, Fe and Zr with a high positive correlation between them; Group 2) Ca, Br

255 and Sr have negative correlation with Group 1. Based on this, the sequence is subdivided in two
256 principal sedimentary units. The lower ~87 cm of the record is designated to Unit 1,
257 characterized principally by relatively low values of MS and higher values of Ca. The upper ~28
258 cm of the sequence is designated to Unit 2, in which the mineralogical composition is lower in
259 Ca with higher values of MS in correlation with mostly siliciclastics elements (Si, K, Ti, Fe and
260 Zr).

261
262 Within these two units, four different facies can be identified by visual inspection and by the
263 elemental geochemical composition and TOC of the sediments. *Facies 1* (115-110 cm depth,
264 ~4700 to 4650 cal yr BP; and 89-80 cm depth ~4300 to 4000 cal yr BP) are characterized by
265 dark brown organic clays that bear charophytes and macroscopic plant remains. They also have
266 depicted relative higher values of TOC values (Fig. 3). *Facies 2* (110-89 cm depth ~4650 to 4300
267 cal yr BP; and 80-42 cm depth, ~4000 to 1600 cal yr BP) is composed of brown clays, with the
268 occurrence of gastropods and charophytes. This facies is also characterized by lower TOC
269 values. *Facies 3* (42-28 cm depth, ~1600 to 450 cal yr BP) is characterized by grayish brown
270 clays with the occurrence of gastropods, and lower values of TOC, and an increasing trend in MS
271 and in siliciclastic elements. *Facies 4* (28-0 cm, ~450 cal yr BP to Present) is made up of light
272 grayish brown clays and features a strong increase in siliciclastic linked to a strong increase in
273 MS.

274 **4.3 Pollen and NPP**

275 Several terrestrial and aquatic pollen taxa were identified but only the most representative taxa
276 are here plotted in the summary pollen diagram (Fig. 4). Selected NPP percentages are also
277 displayed in Figure 4. Four pollen zones (PA) were visually identified with the help of a cluster
278 analysis using the program CONISS (Grimm, 1987). Pollen concentration was higher during
279 Unit 1 with a decreasing trend in the transition to Unit 2 and a later increase during the pollen
280 subzone PA-4b (Fig. 4). Pollen zones are described below:

281 **4.3.1 Zone PA-1 [~4720 to 3400 cal yr BP/ ~2800 to 1450 BCE (115-65 cm)]**

282 Zone 1 is characterized by the abundance of Mediterranean forest species reaching up to ca. 70
283 %. Another important taxon in this zone is *Pinus*, with average values around 18 %. Herbs are
284 largely represented by Poaceae, averaging around 10 %, and reaching up to ca. 25 %. This pollen
285 zone is subdivided into PA-1a, PA-1b and PA-1c (Fig. 4). The principal characteristic that
286 differentiating PA-1a from PA-1b (boundary at ~4650 cal yr BP/~2700 BCE) is the decrease in
287 Poaceae, the increase in *Pinus*, and the appearance of cf. *Vitis*. The subsequent decrease in
288 Mediterranean forest pollen to average values around 40 %, the increase in *Pinus* to average ~25
289 % and a progressive increase in Ericaceae to ~6 to 11 %, distinguishes subzones PA-1b and PA-
290 1c (boundary at ca. 3950 cal yr BP).

291 **4.3.2. Zone PA-2 [~3400 to 1550 cal yr BP/~1450 BCE to 400 CE (65-41 cm)]**

292 The main features of this zone are the increase in Ericaceae up to ~16 % and in deciduous
293 *Quercus*, reaching values ~20 %. Therefore, the Mediterranean forest component progressively
294 declined to values around 34 %. Some herbs, such as Cichorioideae, became more abundant
295 reaching average percentages of ~7 %. This pollen zone can be subdivided in subzones PA-2a

296 and PA-2b with a boundary at ~2850 cal yr BP (~900 BCE). The principal characteristics that
297 differentiate these subzones is marked by the increasing trend in deciduous *Quercus* and
298 Ericaceae. The increase in *Botryococcus*, which averages 4 to 9 %. Also notable is the expansion
299 of *Mougeotia* and *Zygnema* types.

300 **4.3.3 Zone PA-3 [~1550 to 400 cal yr BP/~400 CE to 1550 CE (41-29 cm)]**

301 This zone is distinguished by the continuing decline of Mediterranean forest elements.
302 Cichorioideae reached average values of about 40 %, and is paralleled by the decrease in
303 Ericaceae. A decline in *Botryococcus* and other algal remains is also observed in this zone,
304 although there is an increase in total Thecamoebians from average of <1 % to 10 %. This pollen
305 zone is subdivided in subzones PA-3a and PA-3b at ~1000 cal yr BP (~950 CE). The main
306 features that differentiate these subzones are the increase in *Olea* from subzone PA-3a to PA-3b
307 from average values of ~1 to 5 %. The increasing trend in Poaceae is also a feature in this
308 subzone, as well as the slight increase in Asteroideae at the top. Significant changes are
309 documented in NPP percentages in this subzone with the increase of some fungal remain such as
310 *Tilletia* and *Glomus* type. Furthermore, a decrease in *Botryococcus* and the near disappearance of
311 other algal remains such as *Mougeotia* occurred.

312 **4.3.4 Zone PA-4 [~last 400 cal yr BP/ ~ 1550 CE to Present (29-0 cm)]**

313 The main feature in this zone is the significant increase in *Pinus*, reaching maximum values of
314 ~32 %, an increase in Poaceae to ~40 %) and the decrease in Cichorioideae (~44 to 16 %). Other
315 important changes are the nearly total disappearance of some shrubs such as *Pistacia* and a
316 decreasing trend in Ericaceae, as well as a further decline in Mediterranean forest pollen. An
317 increase in wetland pollen taxa, mostly *Typha*, also occurred. A significant increase in
318 xerophytes, mostly Amaranthaceae to ~14 % is also observed in this period. Other herbs such as
319 *Plantago*, Polygonaceae and Convolvulaceae show moderate increases. PA-4 is subdivided into
320 subzones PA-4a and PA-4b (Fig. 4). The top of the record (PA-4b), which corresponds with the
321 last ~120 yr, is differentiated from subzone PA-4a (from ~400 – 120 cal yr BP) by a decline in
322 some herbs such as Cichorioideae. However, an increase in other herbs such as Amaranthaceae
323 and Poaceae occurred. The increase in *Plantago* is also significant during this period. PA-4b also
324 has a noteworthy increase in *Pinus* (from ~14 to 27 %) and a slight increase in *Olea* and
325 evergreen *Quercus* are also characteristic of this subzone. With respect to NPPs, thecamoebians
326 such as *Arcella* type and in the largely coprophilous sordariaceous (Sordariales) spores also
327 increase. This zone also documents the decrease in fresh-water algal spores, in *Botryococcus*
328 concomitant with *Mougeotia* and *Zygnema* type.

329 **4.4 Estimated lake level reconstruction**

330 Different local proxies from the Padul-15-05 record [Si, Ca, TOC, MS, hygrophytes (Cyperaceae
331 and *Typha*), Poaceae and algae (including *Botryococcus*, *Zygnema* types and *Mougeotia*) groups]
332 have been depicted in order to understand the relationship between lithological, geochemical,
333 and palynological variability and the water lake level oscillations. Sediments with higher values
334 of TOC (more algae and hygrophytes) and rich in Ca (related with the occurrence of shells and
335 charophytes remains) most likely characterized a shallow water environment (Unit 1). The
336 continuous decline in *Botryococcus*, the disappearance of charophytes and the progressively

337 increase in detritics (increase in MS and Si values) could be associated with shallower and even
338 ephemeral lake environment (transition from Unit 1 to Unit 2; ~41 to 28 cm). The absence of
339 aquatic remains, almost disappearance of *Botryococcus* and decreasing Ca and a lower TOC
340 and/or a higher input of clastic material (higher MS and Si values) into the lake, could be related
341 with lake level lowering, and even emerged conditions (increase in Poaceae; Unit 2) (Fig. 5).

342 4.5 Spectral analysis

343 Spectral analysis was performed on selected pollen and NPP time series (Mediterranean forest
344 and *Botryococcus*), as well as TOC in order to identify millennial- and centennial-scale
345 periodicities. The mean sampling resolution for pollen and NPP is ~50 yr and for geochemical
346 data is ~80 yr. Statistically significant cycles, above the 90, 95 and 99 % of confident levels,
347 were found around 800, 680, 300, 240, 200, 170 (Fig. 7).

348 5 Discussion

349 Numerous proxies have been used in this study to interpret the paleoenvironmental and
350 hydrodynamic changes recorded in the Padul sedimentary record during the last 4700 cal yr BP.
351 Palynological analysis (pollen and NPP) is commonly used as a proxy for vegetation and climate
352 change, and lake level variations, as well as human impact and land uses (e.g. Faegri and
353 Iversen, 1990; van Geel et al., 1983). Disentangling natural vs. anthropogenic effects on the
354 environment in the last millennia is sometimes challenging but can be persuaded using a multi-
355 proxy approach (Roberts et al., 2011; Sadori et al., 2011). In this study, we used the variations
356 between Mediterranean forest taxa, xerophytes and algal communities for paleoclimatic
357 variability and the occurrence of nitrophilous and ruderal plant communities and some NPPs for
358 identifying human influence in the study area. Variations in arboreal pollen (AP, including
359 Mediterranean tree species) have previously been used in previous Sierra Nevada records as a
360 proxy for humidity changes (Jiménez-Moreno and Anderson, 2012; Ramos-Román et al., 2016).
361 The increase or decrease in Mediterranean forest species has been used as a proxy for climate
362 change in other studies in the western Mediterranean region, with greater forest development
363 generally meaning higher humidity (Fletcher et al., 2013; Fletcher and Sánchez-Goñi, 2008). On
364 the other hand, increases in xerophyte pollen taxa (i.e., *Artemisia*, *Ephedra*, *Amaranthaceae*)
365 have been used as an indication of aridity in this area (Anderson et al., 2011; Carrión et al.,
366 2007).

367
368 The chlorophyceae alga *Botryococcus* sp. has been used as an indicator of freshwater
369 environments, in relatively productive fens, temporary pools, ponds or lakes (Guy-Ohlson,
370 1992). The high visual and statistical correlation between *Botryococcus* from Padul-15-05 and
371 North Atlantic temperature estimations (Bond et al., 2001; $r = -0.63$; $p < 0.0001$; between ca.
372 4700 to 1500 cal yr BP – the decreasing and very low *Botryococcus* occurrence in the last 1500
373 cal yr BP makes this correlation moderate: $r = -0.48$; $p < 0.0001$ between 4700 and -65 cal yr BP)
374 seems to show that in this case *Botryococcus* is driven by temperature change and would reflect
375 variations in lake productivity (increasing with warmer water temperatures).

376
377 Human impact can be investigated using several palynomorphs. Nitrophilous and ruderal pollen
378 taxa, such as *Convolvulus*, *Plantago lanceolata* type, Urticaceae type and *Polygonum avicularis*
379 type, are often proxies for human impact (Riera et al., 2004), and abundant *Amaranthaceae* has

380 also been used as well (Sadori et al., 2003). Some species of Cichorioideae have been described
381 as nitrophilous taxa (Abel-Schaad and López-Sáez, 2013) and as grazing indicators (Florenzano
382 et al., 2015; Mercuri et al., 2006; Sadori et al., 2016). At the same time, NPP taxa such as some
383 coprophilous fungi, Sordariales and thecamoebians are also used as indicators of anthropization
384 and land use (Carrión et al., 2007; Ejarque et al., 2015; van Geel et al., 1989; Riera et al., 2006).
385 *Tilletia* a grass-parasitizing fungi has been described as an indicator of grass cultivation in other
386 Iberian records (Carrión et al., 2001a). In this study we follow the example of others (van Geel et
387 al., 1989; Morellón et al., 2016; Sadori et al., 2016) who used the NPP soil mycorrhizal fungus
388 *Glomus* sp. as a proxy for erosive activity.

389
390 The palynological analysis, variations in the lithology, geochemistry and macrofossil remains
391 (gastropod shells and charophytes) from the Padul-15-05 core helped us reconstruct the
392 estimated lake level and the local environment changes in the Padul area and their relationship
393 with regional climate (Figs. 5). Several previous studies on Late Holocene lake records from the
394 Iberian Peninsula show that lithological changes can be used as a proxy for lake level
395 reconstruction (Martín-Puertas et al., 2011; Morellón et al., 2009; Riera et al., 2004). For
396 example, carbonate sediments formed by biogenic remains of gastropods and charophytes are
397 indicative of shallow lake waters (Riera et al., 2004). Furthermore, van Geel et al. (1983),
398 described occurrences of *Mougeotia* and *Zygnema* type (Zygnemataceae) as typical of shallow
399 water environments. The increase in organic matter accumulation deduced by TOC (and Br)
400 could be considered as characteristic of high productivity (Kalugin et al., 2007) in these shallow
401 water environments. On the other hand, increases in clastic input in lake sediments have been
402 interpreted as due to lowering of lake level and more influence of terrestrial-fluvial deposition in
403 a very shallow/ephemeral lake (Martín-Puertas et al., 2008). Carrión (2002) related the increase
404 in some fungal species and Asteraceae as indicators of seasonal desiccation stages in lakes.
405 Nevertheless, in natural environments with potential interactions with human activities the
406 increase in clastic deposition related with other indications of soil erosion (e.g. *Glomus* sp.) may
407 be assigned to intensification in land use (Morellón et al., 2016; Sadori et al., 2016).

408 **5.1 Late Holocene aridification trend**

409 Our work confirms the progressive aridification trend that occurred during at least the last ~4700
410 cal yr BP in the southern Iberian Peninsula, as shown here by the progressive decrease in
411 Mediterranean forest component and the increase in herbs (Figs. 4 and 6). Our lake level
412 interpretations agree with the pollen data, showing an overall decrease during the Late Holocene,
413 from a shallow water table containing relatively abundant organic matter (high TOC, indicating
414 higher productivity), gastropods and charophytes (high Ca values) to a low-productive
415 ephemeral/emerged environment (high clastic input and MS and decrease in Ca) (Fig. 5). This
416 natural progressive aridification confirmed by the decrease in Mediterranean forest taxa and
417 increase in siliciclastics pointing to a change towards ephemeral (even emerged) environments
418 became more prominent since about 1550 cal yr BP and then enhanced again since ca. 400 cal yr
419 BP to Present. A clear increase in human land use is also observed during the last ca. 1550 cal yr
420 BP (see below), including abundant *Glomus* from erosion, which shows that humans were at
421 least partially responsible for this sedimentary change.

422 A suite of proxies previous studies supports our conclusions regarding the aridification trend
423 since the Middle Holocene (Carrión, 2002; Carrión et al., 2010; Fletcher et al., 2013; Fletcher
424 and Sánchez-Goñi, 2008; Jiménez-Espejo et al., 2014; Jiménez-Moreno et al., 2015). In the

425 western Mediterranean region the decline in forest development during the Middle and Late
426 Holocene is related with a decrease in summer insolation (Fletcher et al., 2013; Jiménez-Moreno
427 and Anderson, 2012), which may have decreased winter rainfall as a consequence of a northward
428 shift of the westerlies - a long-term enhanced positive NAO trend – which induced drier
429 conditions in this area since 6000 cal yr BP (Magny et al., 2012). Furthermore, the decrease in
430 summer insolation would produce a progressive cooling, with a reduction in the length of the
431 growing season as well as a decrease in the sea-surface temperature (Marchal et al., 2002),
432 generating a decrease in the land-sea contrast that would be reflected in a reduction of the wind
433 system and a reduced precipitation gradient from sea to shore during the fall-winter season. The
434 aridification trend can clearly be seen in the nearby alpine records from the Sierra Nevada, where
435 there was little influence by human activity (Anderson et al., 2011; Jiménez-Moreno et al., 2013;
436 Jiménez-Moreno and Anderson, 2012; Ramos-Román et al., 2016).

437 **5.2 Millennial- and centennial-scale climate variability in the Padul peat bog during the** 438 **Late Holocene**

439 The multi-proxy paleoclimate record from Padul-15-05 shows an overall aridification trend.
440 However, this trend seems to be modulated by millennial- and centennial-scale climatic
441 variability.

442 **5.2.1 Aridity pulses around 4200 (4500, 4300 and 4000 cal yr BP) and around 3000 cal yr** 443 **BP (3300 and 2800 cal yr BP)**

444 Marked aridity pulses are registered in the Padul-15-05 record around 4200 and 3000 cal yr BP
445 (Unit 1; PA-1 and PA-2a; Figs. 6 and 7). These arid pulses are mostly evidenced in this record by
446 declines in Mediterranean forest taxa, as well as lake level drops and/or cooling evidenced by a
447 decrease in organic component as TOC and the decrease in *Botryococcus* algae. However, a
448 discrepancy between the local and regional occurs between 3000-2800 cal yr BP, with an
449 increase in the estimated lake level and a decrease in the Mediterranean forest during the late
450 Bronze Age until the early Iron Age (Figs. 6 and 7). The disagreement could be due to
451 deforestation by humans during a very active period of mining in the area observed as a peak in
452 lead pollution in the alpine records from Sierra Nevada (García-Alix et al., 2013). The aridity
453 pulses agree regionally with recent studies carried out at higher elevation in the Sierra Nevada,
454 a decrease in AP percentage in Borreguil de la Caldera record around 4000-3500 cal yr BP
455 (Ramos-Román et al., 2016), high percentage of non-arboreal pollen around 3400 cal ka BP in
456 Zoñar lake [Southern Córdoba Natural Reserve; (Martín-Puertas et al., 2008)], and lake
457 desiccation at ca. 4100 and 2900 cal yr BP in Lake Siles (Carrión et al., 2007). Jalut et al. (2009)
458 compared paleoclimatic records from different lakes in the western Mediterranean region and
459 also suggested a dry phase between 4300 to 3400 cal yr BP, synchronous with this aridification
460 phase. Furthermore, in the eastern Mediterranean basin other pollen studies show a decrease in
461 arboreal pollen concentration toward more open landscapes around 4 cal ka BP (Magri, 1999).

462
463 Significant climatic changes also occurred in the Northern Hemisphere at those times and polar
464 cooling and tropical aridity are observed at ca. 4200-3800 and 3500-2500 cal yr BP; (Mayewski
465 et al., 2004), cold events in the North Atlantic [cold event 3 and 2; (Bond et al., 2001)], decrease
466 in solar irradiance (Steinhilber et al., 2009) and humidity decreases in the eastern Mediterranean
467 area at 4200 cal yr BP (Bar-Matthews et al., 2003) that could be related with global scale climate

468 variability (Fig. 6). These generally dry phases between 4.5 and 2.8 in Padul-15-05 are generally
469 in agreement with persistent positive NAO conditions during this time (Olsen et al., 2012).
470 The high-resolution Padul-15-05 record shows that climatic crises such as the essentially global
471 event at ~4200 cal yr BP (Booth et al., 2005), are actually multiple events in climate variability
472 at centennial-scales (i.e., ca. 4500, 4300, 4000 cal yr BP).

473 **5.2.2 Iberian-Roman Humid Period (~2600 to 1600 cal yr BP)**

474 High relative humidity is recorded in the Padul-15-05 record between ca. 2600 and 1600 cal yr
475 BP, synchronous with the well-known Iberian-Roman Humid Period (IRHP; between 2600 and
476 1600 cal yr BP; (Martín-Puertas et al., 2009). This is interpreted in our record due to an increase
477 in the Mediterranean forest species at that time (Unit 1; PA-2b; Figs. 6 and 7). In addition, there
478 is a simultaneous increase in *Botryococcus* algae, which is probably related to higher
479 productivity during warmer conditions and relatively higher water level. Evidence of a wetter
480 climate around this period has also been shown in several alpine records from Sierra Nevada. For
481 example, in the Laguna de la Mula core (Jiménez-Moreno et al. 2013) an increase in deciduous
482 *Quercus* is correlated with the maximum in algae between 2500 to 1850 cal yr BP, also
483 evidencing the most humid period of the Late Holocene. A geochemical study from the Laguna
484 de Río Seco (also in Sierra Nevada) also evidenced humid conditions around 2200 cal yr BP by
485 the decrease in Saharan dust input and the increase in detritic sedimentation into the lake
486 suggesting higher rainfall (Jiménez-Espejo et al., 2014). In addition, Ramos-Román et al. (2016)
487 showed an increase in AP in the Borreguil de la Caldera record around 2200 cal yr BP,
488 suggesting an increase in humidity at that time.

489
490 Other records from the Iberian Peninsula also show this pattern to wetter conditions during the
491 IRHP. For example, high lake levels are recorded in Zoñar Lake in southern Spain between 2460
492 to 1600 cal yr BP, only interrupted by a relatively arid pulse between 2140 and 1800 cal yr BP
493 (Martín-Puertas et al., 2009). An increase in rainfall is described in the central region of the
494 Iberian Peninsula in a study from the Tablas de Daimiel National Park between 2100 and 1680
495 cal yr BP (Gil García et al., 2007). Deeper lake levels at around 2650 to 1580 cal yr BP, also
496 interrupted by an short arid event at ca. 2125-1790 cal yr BP, were observed to the north, in the
497 Iberian Range (Currás et al., 2012). The fact that the Padul-15-05 record also shows a relatively
498 arid-cold event between 2150-2050 cal yr BP, just in the middle of this relative humid-warm
499 period, seems to point to a common feature of centennial-scale climatic variability in many
500 western Mediterranean and North Atlantic records (Fig. 6). Humid climate conditions at around
501 2500 cal yr BP are also interpreted in previous studies from lake level reconstructions from
502 Central Europe (Magny, 2004). Increases in temperate deciduous forest are also observed in
503 marine records from the Alboran Sea around 2600 to 2300 cal yr BP, also pointing to high
504 relative humidity (Combourieu-Nebout et al., 2009; Fletcher et al., 2007). Overall humid
505 conditions between 2600 and 1600 cal yr BP seem to agree with predominant negative NAO
506 reconstructions at that time, which would translate into greater winter (and thus more effective)
507 precipitation in the area triggering greater development of forest species in the area.

508
509 Generally warm conditions are interpreted between 1900 and 1700 cal yr BP in the
510 Mediterranean Sea, with high sea surface temperatures (SSTs), and in the North Atlantic area,
511 with the decrease in Drift Ice Index. In addition, persistent positive solar irradiance occurred at
512 that time. The increase in *Botryococcus* algae reaching maxima during the IRHP also seems to

513 point to very productive and perhaps warmer conditions in the Padul peat bog area (Fig. 6).

514 **5.2.3 DA and MCA (~1550 cal yr BP to 600 cal yr BP)**

515 Enhanced aridity occurred right after the IRHP in the Padul peat bog area. This is deduced in the
516 Padul-15-05 record by a significant forest decline, with a prominent decrease in Mediterranean
517 forest elements, an increase in herbs (Unit 1; PA-3; Figs. 4 and 7). In addition, our evidence
518 suggests a transition from a shallow lake to a more ephemeral wetland. This is suggested by the
519 disappearance of charophytes, a significant decrease in algae component and higher Si and MS
520 and lower TOC values (Unit 1; Figs. 6 and 7). Humans probably also contributed to enhancing
521 erosion in the area during this last ~1550 cal yr BP. The significant change during the transition
522 from Unit 1 to Unit 2 with a decrease in the pollen concentration and the increase in
523 Cichoroideae could be due to enhanced pollen degradation as Cichoroideae have been found to
524 be very resistant to pollen deterioration (Bottema, 1975). However, the occurrence of other
525 pollen taxa (e.g. *Quercus*, Ericaceae, *Pinus*, Poaceae, *Olea*) showing climatic trends and
526 increasing between ca. 1500-400 cal yr BP and a decrease in Cichoroideae in the last ~400 cal yr
527 BP, when an increase in clastic material occurred, do not entirely support a preservation issue
528 (see section of Human activity; 5.4).

529
530 This phase could be separated into two different periods. The first period occurred between
531 ~1550 cal yr BP and 1100 cal yr BP (~400 to 900 CE) and is characterized by a decreasing trend
532 in Mediterranean forest and *Botryococcus* taxa. This period corresponds with the Dark Ages
533 [from ca. 500 to 900 CE; (Moreno et al., 2012)]. Correlation between the decline in
534 Mediterranean forest, the increase in the Drift Ice Index in the North Atlantic record (cold event
535 1; Bond et al., 2001), the decline in SSTs in the Mediterranean Sea and maxima in positive NAO
536 reconstructions suggests drier and colder conditions during this time (Fig. 6). Other
537 Mediterranean and central-European records agree with our climate interpretations, for example,
538 a decrease in forest pollen types is shown in a marine record from the Alboran Sea (Fletcher et
539 al., 2013) and a decrease in lake levels is also observed in Central Europe (Magny et al., 2004)
540 pointing to aridity during the DA. Evidences of aridity during the DA have been shown too in the
541 Mediterranean part of the Iberian Peninsula, for instance, cold and arid conditions were
542 suggested in the northern Betic Range by the increase in xerophytic herbs around 1450 and 750
543 cal yr BP (Carrión et al., 2001b) and in southeastern Spain by a forest decline in lacustrine
544 deposits around 1620 and 1160 cal yr BP (Carrión et al., 2003). Arid and colder conditions
545 during the Dark Ages (around 1680 to 1000 cal yr BP) are also suggested for the central part of
546 the Iberian Peninsula using a multiproxy study of a sediment record from the Tablas de Daimiel
547 Lake (Gil García et al., 2007).

548
549 A second period that we could differentiate occurred around 1100 to 600 cal yr BP/900 to 1350
550 CE, during the well-known MCA (900 to 1300 CE after Moreno et al., 2012). During this period
551 the Padul-15-05 record shows a slight increasing trend in the Mediterranean forest taxa with
552 respect to the DA, but the decrease in *Botryococcus* and the increase in herbs still point to overall
553 arid conditions. This change could be related to an increase in temperature, favoring the
554 development of temperate forest species, and would agree with inferred increasing temperatures
555 in the North Atlantic areas, as well as the increase in solar irradiance and the increase in SSTs in
556 the Mediterranean Sea (Fig.7). This hypothesis would agree with the reconstruction of persistent
557 positive NAO and overall warm conditions during the MCA in the western Mediterranean (see

558 synthesis in Moreno et al., 2012). A similar pattern of increasing xerophytic vegetation during
559 the MCA is observed in alpine peat bogs and lakes in the Sierra Nevada (Anderson et al., 2011;
560 Jiménez-Moreno et al., 2013; Ramos-Román et al., 2016) and arid conditions are shown to occur
561 during the MCA in southern and eastern Iberian Peninsula deduced by increases in salinity and
562 lower lake levels (Corella et al., 2013; Martín-Puertas et al., 2011). However, humid conditions
563 have been reconstructed for the northwestern of the Iberian Peninsula at this time (Lebreiro et al.,
564 2006; Moreno et al., 2012), as well as northern Europe (Martín-Puertas et al., 2008). The
565 different pattern of precipitation between northwestern Iberia / northern Europe and the
566 Mediterranean area is undoubtedly a function of the NAO precipitation dipole (Trouet et al.,
567 2009).

568 **5.2.4 The last ~600 cal yr BP: LIA (~600 to 100 cal yr BP/~1350 to 1850 CE) and IE (~100** 569 **cal yr BP to Present/~1850 CE-Present)**

570 Two climatically distinct periods can be distinguished during the last ca. 600 years (end of PA-
571 3b to PA-4; Fig. 4) in the area. However, the climatic signal is more difficult to interpret due to a
572 higher human impact at that time. The first phase around 600-500 cal yr BP was characterized as
573 increasing relative humidity by the decrease in xerophytes and the increase in Mediterranean
574 forest taxa and *Botryococcus* after a period of decrease during the DA and MCA, corresponding
575 to the LIA. The second phase is characterized here by the decrease in the Mediterranean forest
576 around 300-100 cal yr BP, pointing to a return to more arid conditions during the last part of the
577 LIA (Figs. 4 and 7). This climatic pattern agrees with an increase in precipitation by the
578 transition from positive to negative NAO mode and from warmer to cooler conditions in the
579 North Atlantic area during the first phase of the LIA and a second phase characterized by cooler
580 (cold event 0; Bond et al., 2001) and drier conditions (Fig. 6). A stronger variability in the SSTs
581 is described in the Mediterranean Sea during the LIA (Fig. 6). Mayewski et al. (2004) described
582 a period of climate variability during the Holocene at this time (600 to 150 cal yr BP) suggesting
583 a polar cooling but more humid in some parts of the tropics. Regionally, (Morellón et al., 2011)
584 also described a phase of more humid conditions between 1530 to 1750 CE (420 to 200 cal yr
585 BP) in a lake sediment record from NE Spain. An alternation between wetter to drier periods
586 during the LIA are also shown in the nearby alpine record from Borreguil de la Caldera in the
587 Sierra Nevada mountain range (Ramos-Román et al., 2016).

588 The environmental transition from ephemeral, observed in the last ca. 1550 cal yr BP (Unit 1;
589 Fig. 5), to emerged conditions in the last ca. 400 cal yr BP. This is shown by the highest MS and
590 Si values the increase in wetland plants and the stronger decrease in Ca and organic components
591 (TOC) in the sediments in the uppermost part of the Padul-15-05 record (Unit 2; Figs. 3 and 6).

592 **5.3 Centennial-scale variability**

593 Time series analysis has become important in determining the recurrent periodicity of cyclical
594 oscillations in paleoenvironmental sequences (e.g. Jiménez-Espejo et al., 2014; Ramos-Román et
595 al., 2016; Rodrigo-Gámiz et al., 2014; Fletcher et al., 2013). This analysis also assists in
596 understanding possible relationships between the paleoenvironmental proxy data and the
597 potential triggers of the observed cyclical changes: i.e., solar activity, atmospheric, oceanic
598 dynamics and climate evolution during the Holocene. The cyclostratigraphic analysis on the
599 pollen (Mediterranean forest; regional signal), algae (*Botryococcus*; local signal) and TOC (local
600 signal) times series from the Padul-15-05 record evidence centennial-scale cyclical patterns with

601 periodicities around ~800, 680, 300, 240, 200 and 170 years above the 90 % confidence levels
602 (Fig. 7).

603
604 Previous cyclostratigraphic analysis in Holocene western Mediterranean records suggest cyclical
605 climatic oscillations with periodicities around 1500 and 1750 yr (Fletcher et al., 2013; Jiménez-
606 Espejo et al., 2014; Rodrigo-Gámiz et al., 2014). Other North Atlantic and Mediterranean
607 records also present cyclicities in their paleoclimatic proxies of ca. 1600 yr (Bond et al., 2001;
608 Debret et al., 2007; Rodrigo-Gámiz et al., 2014). However, this cycle is absent from the
609 cyclostratigraphic analysis in the Padul-15-05 record (Fig. 7). In contrast, the spectral analysis
610 performed in the Mediterranean forest time series from Padul peat bog record, pointing to
611 cyclical hydrological changes, shows a significant ~800 yr cycle that could be related to solar
612 variability (Damon and Sonett, 1991) or could be the second harmonic of the ca. ~1600 yr
613 oceanic-related cycle (Debret et al., 2009). A very similar periodicity of ca. 760 yr is detected in
614 the *Pinus* forest taxa, also pointing to humidity variability, from the alpine Sierra Nevada site of
615 Borreguil de la Caldera and seems to show that this is a common feature of cyclical
616 paleoclimatic oscillation in the area.

617
618 A significant ~680 cycle is shown in the *Botryococcus* time series most likely suggesting
619 recurrent centennial-scale changes in temperature (productivity) and water availability. A similar
620 cycle is shown in the *Artemisia* signal in an alpine record from Sierra Nevada (Ramos-Román et
621 al., 2016). This cycle around ~650 yr is also observed in a marine record from the Alboran Sea,
622 and was interpreted as the secondary harmonic of the 1300 yr cycle that those authors related
623 with cyclic thermohaline circulation and sea surface temperature changes (Rodrigo-Gámiz et al.,
624 2014).

625
626 A statistically significant ~300 yr cycle is shown in the Mediterranean forest taxa and TOC from
627 the Padul-15-05 record suggesting shorter-scale variability in water availability. This cycle is
628 also observed in the cyclical *Pinus* pollen data from Borreguil de la Caldera at higher elevations
629 in the Sierra Nevada (Ramos-Román et al., 2016). This cycle could be principally related to
630 NAO variability as observed by Olsen et al. (2012), which follows variations in humidity
631 observed in the Padul-15-05 record. NAO variability also regulates modern precipitation in the
632 area.

633
634 The *Botryococcus* and TOC time series shows variability with a periodicity around ~240, 200
635 and 164 yrs. Sonett and Suess, (1984) described a significant cycle in solar activity around ~208
636 yr (Suess solar cycle), which could have triggered our ~200 cyclicity. The observed ~240 yr
637 periodicity in the Padul-15-05 record could be either related to variations in solar activity or due
638 to the mixed effect of the solar together with the ~300 yr NAO-interpreted cycle and could point
639 to a solar origin of the centennial-scale NAO variations as suggested by previously published
640 research (Lukianova and Alekseev, 2004; Zanchettin et al., 2008). Finally, a significant ~170 yr
641 cycle has been observed in both the Mediterranean forest taxa and *Botryococcus* times series
642 from the Padul-15-05 record. A similar cycle (between 168-174 yr) was also described in the
643 alpine pollen record from Borreguil de la Caldera in Sierra Nevada (Ramos-Román et al., 2016),
644 which shows that it is a significant cyclical pattern in climate, probably precipitation, in the area.
645 This cycle could be related to the previously described ~170 yr cycle in the NAO index (Olsen et
646 al., 2012), which would agree with the hypothesis of the NAO controlling millennial- and

647 centennial-scale environmental variability during the Late Holocene in the area (García-Alix et
648 al., 2017; Ramos-Román et al., 2016).

649 **5.4 Human activity**

650 Humans probably had an impact in the area since Prehistoric times, however, the Padul-15-05
651 multiproxy record shows a more significant human impact during the last ca. 1550 cal yr BP,
652 which intensified in the last ~500 years (since 1450 CE to Present). This is deduced by, a
653 significant increase in nitrophilous plant taxa such as Cichorioideae, Convolvulaceae,
654 Polygonaceae and *Plantago* and the increase in some NPP such as *Tilletia*, coprophilous fungi
655 and thecamoebians (Unit 2; PA-4; Fig. 4). Most of these pollen taxa and NPPs are described in
656 other southern Iberian paleoenvironmental records as indicators of land uses, for instance,
657 *Tilletia* and covarying nitrophilous plants have been described as indicators of farming (e.g.
658 Carrión et al., 2001a). Thecamoebians also show a similar trend and have also been detected in
659 other areas being related to nutrient enrichment as consequences of livestock (Fig. 8). The
660 stronger increase in Cichorioideae have also been described as indicators of animal grazing in
661 areas subjected to intense use of the territory (Mercuri et al., 2006). Interestingly, these taxa
662 began to decline around ca. 400 cal yr BP (~1550 CE), coinciding with the higher increase in
663 detritic material into the basin. We could then interpreted this increase in Cichorioideae as
664 greater in livestock activity in the surroundings of the lake during this period, which is supported
665 by the increase in these other proxies related with animal husbandry.

666

667 Climatically, this event coincides with the start of persistent negative NAO conditions in the area
668 (Trouet et al., 2009), which could have further triggered more rainfall and more detritic input
669 into the basin. (Bellin et al., 2011) in a study from the Betic Cordillera (southern Iberian
670 Peninsula) demonstrate that soil erosion increase in years with higher rainfall and this could be
671 intensified by human impact. Nevertheless, in a study in the southeastern part of the Iberian
672 Peninsula (Bellin et al., 2013) suggested that major soil erosion could have occurred by the
673 abandonment of agricultural activities in the mountain areas as well as the abandonment of
674 irrigated terrace systems during the Christian Reconquest. Enhanced soil erosion at this time is
675 also supported by the increase in *Glomus* type (Fig. 4).

676

677 An important change in the sedimentation in the environment is observed during the last ca. 400
678 cal yr BP marked by the stronger increase in MS and Si values. This higher increase in detritics
679 occurred during an increase in other plants related with human and land uses such as
680 Polygonaceae, Amaranthaceae, Convolvulaceae, *Plantago*, Apiaceae and Cannabaceae-
681 Urticaceae type (Land Use Plants; Fig. 8). This was probably related to drainage canals in the
682 Padul peat bog in the late XVIII century for cultivation purposes (Villegas Molina, 1967). The
683 increase in wetland vegetation and higher values of Poaceae could be due to cultivation of
684 cereals or by an increase in the population of *Phragmites australis* (also a Poaceae), very
685 abundant in the Padul peat bog margins at present due to the increase in drained land surface.

686 The uppermost part (last ca. 100 cal yr BP) of the pollen record from Padul-15-05 shows an
687 increasing trend in some arboreal taxa at that time, including Mediterranean forest, *Olea* and
688 *Pinus* (Fig. 4). This change is most likely of human origin and generated by the increase in *Olea*
689 cultivation in the last two centuries, also observed in many records from higher elevation sites
690 from Sierra Nevada, and *Pinus* and other Mediterranean species reforestation in the 20th century
691 (Anderson et al., 2011; Jiménez-Moreno and Anderson, 2012; Jiménez-Moreno et al., 2013;

692 Ramos-Román et al., 2016).

693 **6 Conclusions**

694 Our multiproxy analysis from the Padul-15-05 sequence has provided a detailed climate
695 reconstruction for the last 4700 ca yr BP for the Padul peat bog area and the western
696 Mediterranean. This study, supported by the comparison with other Mediterranean and North
697 Atlantic records suggests a link between vegetation, atmospheric dynamics and insolation and
698 solar activity during the Late Holocene. A climatic aridification trend occurred during the Late
699 Holocene in the Sierra Nevada and the western Mediterranean, probably linked with an orbital-
700 scale declining trend in summer insolation. This long-term trend is modulated by centennial-
701 scale climate variability as shown by the pollen (Mediterranean forest taxa), algae
702 (*Botryococcus*) and sedimentary and geochemical data in the Padul record. These events can be
703 correlated with regional and global scale climate variability. Cold and arid pulses identified in
704 this study around the 4200 and 3000 cal yr BP are synchronous with cold events recorded in the
705 North Atlantic and decreases in precipitation in the Mediterranean area, probably linked to
706 persistent positive NAO mode. Moreover, one of the most important humid and warmer periods
707 during the Late Holocene in the Padul area coincides in time with the well-known IRHP,
708 characterized by warm and humid conditions in the Mediterranean and North Atlantic regions
709 and overall negative NAO conditions. A drastic decline in Mediterranean forest taxa, trending
710 towards an open landscape and pointing to colder conditions with enhanced aridity, occurred in
711 two steps (DA and end of the LIA) during the last ~1550 cal yr BP. However, this trend was
712 slightly superimposed by a more arid but warmer event coinciding with the MCA and a cold but
713 wetter event during the first part of the LIA. Besides natural climatic and environmental
714 variability, strong evidences exists for intense human activities in the area during the last the last
715 ~1550 years. This suggests that the natural aridification trend during the Late Holocene, which
716 produced a progressive decrease in the Mediterranean forest taxa in the Padul area, could have
717 been intensified by human activities, notably in the last centuries.
718 Furthermore, time series analyses done in the Padul-15-05 record show centennial-scale changes
719 in the environment and climate that are coincident with the periodicities observed in solar,
720 oceanic and NAO reconstructions and could show a close cause-and-effect linkage between
721 them.

722 **Acknowledgements**

723 This work was supported by the project P11-RNM-7332 funded by Consejería de Economía,
724 Innovación, Ciencia y Empleo de la Junta de Andalucía, the project CGL2013-47038-R funded
725 by Ministerio de Economía y Competitividad of Spain and fondo Europeo de desarrollo regional
726 FEDER and the research group RNM0190 (Junta de Andalucía). M. J. R.-R. acknowledges the
727 PhD funding provided by Consejería de Economía, Innovación, Ciencia y Empleo de la Junta de
728 Andalucía (P11-RNM-7332). J.C. acknowledges the PhD funding provided by Ministerio de
729 Economía y Competitividad (CGL2013-47038-R). A.G.-A. was also supported by a Ramón y
730 Cajal Fellowship RYC-2015-18966 of the Spanish Government (Ministerio de Economía y
731 Competitividad). Javier Jaimez (CIC-UGR) is thanked for graciously helping with the coring, the
732 drilling equipment and logistics. We also would like to thanks to the editor (Nathalie
733 Combourieu-Nebout) and Graciela Gil-Romera, Laura Sadori and an anonymous reviewer for
734 their comments and suggestions which improved the manuscript.

735 **References**

- 736 Abel-Schaad, D. and López-Sáez, J. A.: Vegetation changes in relation to fire history and human
737 activities at the Peña Negra mire (Bejar Range, Iberian Central Mountain System, Spain) during
738 the past 4,000 years, *Veg. Hist. Archaeobotany*, 22(3), 199–214, doi:10.1007/s00334-012-0368-
739 9, 2013.
- 740 Alfaro, P., Galinod-Zaldievar, J., Jabaloy, A., López-Garrido, A. C. and Sanz de Galdeano, C.:
741 Evidence for the activity and paleoseismicity of the Padul fault (Betic Cordillera, Southern Spain)
742 [Evidencias de actividad y paleosismicidad de la falla de Padul (Cordillera Bética, sur de
743 España)], *Acta Geol. Hisp.*, 36(3–4), 283–297, 2001.
- 744 Alpert, P., Baldi, M., Ilani, R., Krichak, S., Price, C., Rodó, X., Saaroni, H., Ziv, B., Kishcha, P.,
745 Barkan, J., Mariotti, A. and Xoplaki, E.: Chapter 2 Relations between climate variability in the
746 Mediterranean region and the tropics: ENSO, South Asian and African monsoons, hurricanes
747 and Saharan dust, *Dev. Earth Environ. Sci.*, 4(C), 149–177, doi:10.1016/S1571-9197(06)80005-4,
748 2006.
- 749 Anderson, R. S., Jiménez-Moreno, G., Carrión, J. S. and Pérez-Martínez, C.: Postglacial history of
750 alpine vegetation, fire, and climate from Laguna de Río Seco, Sierra Nevada, southern Spain,
751 *Quat. Sci. Rev.*, 30(13–14), 1615–1629, doi:https://doi.org/10.1016/j.quascirev.2011.03.005,
752 2011.
- 753 Bar-Matthews, M., Ayalon, A., Gilmour, M., Matthews, A. and Hawkesworth, C. J.: Sea–land
754 oxygen isotopic relationships from planktonic foraminifera and speleothems in the Eastern
755 Mediterranean region and their implication for paleorainfall during interglacial intervals,
756 *Geochim. Cosmochim. Acta*, 67(17), 3181–3199, doi:https://doi.org/10.1016/S0016-
757 7037(02)01031-1, 2003.
- 758 Bellin, N., Vanacker, V., van Wesemael, B., Solé-Benet, A. and Bakker, M. M.: Natural and
759 anthropogenic controls on soil erosion in the internal betic Cordillera (southeast Spain), *Catena*,
760 87(2), 190–200, doi:10.1016/j.catena.2011.05.022, 2011.
- 761 Bellin, N., Vanacker, V. and De Baets, S.: Anthropogenic and climatic impact on Holocene
762 sediment dynamics in SE Spain: A review, *Quat. Int.*, 308–309, 112–129,
763 doi:10.1016/j.quaint.2013.03.015, 2013.
- 764 Beug, H.-J.: *Leitfaden der Pollenbestimmung für Mitteleuropa und angrenzende Gebiete*, Fisch.
765 Stuttgart., 61, 2004.
- 766 Blaauw, M.: Methods and code for “classical” age-modelling of radiocarbon sequences, *Quat.*
767 *Geochronol.*, 5(5), 512–518, doi:https://doi.org/10.1016/j.quageo.2010.01.002, 2010.
- 768 Bond, G., Kromer, B., Beer, J., Muscheler, R., Evans, M. N., Showers, W., Hoffmann, S., Lotti-
769 Bond, R., Hajdas, I. and Bonani, G.: Persistent Solar Influence on North Atlantic Climate During
770 the Holocene, *Science*, 294(5549), 2130, doi:10.1126/science.1065680, 2001.

- 771 Booth, R. K., Jackson, S. T., Forman, S. L., Kutzbach, J. E., E. A. Bettis, I., Kreigs, J. and Wright, D.
772 K.: A severe centennial-scale drought in midcontinental North America 4200 years ago and
773 apparent global linkages, *The Holocene*, 15(3), 321–328, doi:10.1191/0959683605hl825ft,
774 2005.
- 775 Bottema, S.: The interpretation of pollen spectra from prehistoric settlements (with special
776 attention of *Liguliflorae*), *Palaeohistoria*, 17, 17–35, 1975.
- 777 Carrión, J. S.: Patterns and processes of Late Quaternary environmental change in a montane
778 region of southwestern Europe, *Quat. Sci. Rev.*, 21(18–19), 2047–2066,
779 doi:[https://doi.org/10.1016/S0277-3791\(02\)00010-0](https://doi.org/10.1016/S0277-3791(02)00010-0), 2002.
- 780 Carrión, J. S., Munuera, M., Dupré, M. and Andrade, A.: Abrupt vegetation changes in the
781 Segura Mountains of southern Spain throughout the Holocene, *J. Ecol.*, 89(5), 783–797,
782 doi:10.1046/j.0022-0477.2001.00601.x, 2001b.
- 783 Carrión, J. S., Andrade, A., Bennett, K. D., Navarro, C. and Munuera, M.: Crossing forest
784 thresholds: inertia and collapse in a Holocene sequence from south-central Spain, *The*
785 *Holocene*, 11(6), 635–653, doi:10.1191/09596830195672, 2001a.
- 786 Carrión, J. S., Fernández, S., Jiménez-Moreno, G., Fauquette, S., Gil-Romera, G., González-
787 Sampérez, P. and Finlayson, C.: The historical origins of aridity and vegetation degradation in
788 southeastern Spain, *J. Arid Environ.*, 74(7), 731–736,
789 doi:<https://doi.org/10.1016/j.jaridenv.2008.11.014>, 2010.
- 790 Carrión, J. S., Sánchez-Gómez, P., Mota, J. F., Yll, R. and Chaín, C.: Holocene vegetation
791 dynamics, fire and grazing in the Sierra de Gádor, southern Spain, *Holocene*, 13(6), 839–849,
792 doi:10.1191/0959683603hl662rp, 2003.
- 793 Carrión, J. S., Fuentes, N., González-Sampérez, P., Quirante, L. S., Finlayson, J. C., Fernández, S.
794 and Andrade, A.: Holocene environmental change in a montane region of southern Europe with
795 a long history of human settlement, *Quat. Sci. Rev.*, 26(11–12), 1455–1475,
796 doi:<https://doi.org/10.1016/j.quascirev.2007.03.013>, 2007.
- 797 Combourieu-Nebout, N., Peyron, O., Dormoy, I., Desprat, S., Beaudouin, C., Kotthoff, U. and
798 Marret, F.: Rapid climatic variability in the west Mediterranean during the last 25 000 years
799 from high resolution pollen data, *Clim Past*, 5(3), 503–521, doi:10.5194/cp-5-503-2009, 2009.
- 800 Corella, J. P., Stefanova, V., El Anjoumi, A., Rico, E., Giralt, S., Moreno, A., Plata-Montero, A. and
801 Valero-Garcés, B. L.: A 2500-year multi-proxy reconstruction of climate change and human
802 activities in northern Spain: The Lake Arreo record, *Palaeogeogr. Palaeoclimatol. Palaeoecol.*,
803 386, 555–568, doi:10.1016/j.palaeo.2013.06.022, 2013.
- 804 Currás, A., Zamora, L., Reed, J. M., García-Soto, E., Ferrero, S., Armengol, X., Mezquita-Joanes,
805 F., Marqués, M. A., Riera, S. and Julià, R.: Climate change and human impact in central Spain

806 during Roman times: High-resolution multi-proxy analysis of a tufa lake record (Somolinos,
807 1280m asl), *Catena*, 89(1), 31–53, doi:10.1016/j.catena.2011.09.009, 2012.

808 Damon, P. E. and Sonett, C. P.: Solar and terrestrial components of the atmospheric C-14
809 variation spectrum. In: Sonett, C.P., Giampapa, M.S., Matthews, M.S. (Eds.), *The Sun in Time*.
810 University of Arizona Press, Tucson, AZ, USA., 1991.

811 Debret, M., Bout-Roumazelles, V., Grousset, F., Desmet, M., McManus, J. F., Massei, N., Sebag,
812 D., Petit, J.-R., Copard, Y. and Trentesaux, A.: The origin of the 1500-year climate cycles in
813 holocene north-atlantic records, *Clim. Past*, 3(4), 569–575, 2007.

814 Debret, M., Sebag, D., Crosta, X., Massei, N., Petit, J.-R., Chapron, E. and Bout-Roumazelles, V.:
815 Evidence from wavelet analysis for a mid-Holocene transition in global climate forcing, *Quat.*
816 *Sci. Rev.*, 28(25–26), 2675–2688, doi:https://doi.org/10.1016/j.quascirev.2009.06.005, 2009.

817 Delgado, J., Alfaro, P., Galindo-Zaldivar, J., Jabaloy, A., Lopez Garrido, A. and Sanz de Galdeano,
818 C.: Structure of the Padul-Nigüelas basin (S Spain) from H/V ratios of ambient noise: application
819 of the method to study peat and coarse sediments, *Pure Appl. Geophys.*, 159(11), 2733–2749,
820 2002.

821 Domingo-García, M., Fernández-Rubio, R., Lopez, J. and González, C.: Aportación al
822 conocimiento de la Neotectónica de la Depresión del Padul (Granada), *Tecniterrae*, 53, 6–16,
823 1983.

824 Ejarque, A., Anderson, R. S., Simms, A. R. and Gentry, B. J.: Prehistoric fires and the shaping of
825 colonial transported landscapes in southern California: A paleoenvironmental study at Dune
826 Pond, Santa Barbara County, *Quat. Sci. Rev.*, 112, 181–196,
827 doi:https://doi.org/10.1016/j.quascirev.2015.01.017, 2015.

828 Faegri, K. and Iversen, J.: *Textbook of Pollen Analysis*. Wiley, New York., 1989.

829 Fletcher, W. J. and Sánchez-Goñi, M. F.: Orbital- and sub-orbital-scale climate impacts on
830 vegetation of the western Mediterranean basin over the last 48,000 yr, *Quat. Res.*, 70(3), 451–
831 464, doi:10.1016/j.yqres.2008.07.002, 2008.

832 Fletcher, W. J., Debret, M. and Sánchez-Goñi, M. F.: Mid-Holocene emergence of a low-
833 frequency millennial oscillation in western Mediterranean climate: Implications for past
834 dynamics of the North Atlantic atmospheric westerlies, *The Holocene*, 23(2), 153–166,
835 doi:10.1177/0959683612460783, 2013.

836 Florenzano, A., Marignani, M., Rosati, L., Fascetti, S. and Mercuri, A. M.: Are Cichorieae an
837 indicator of open habitats and pastoralism in current and past vegetation studies?, *Plant*
838 *Biosyst. - Int. J. Deal. Asp. Plant Biol.*, 149(1), 154–165, doi:10.1080/11263504.2014.998311,
839 2015.

840 Florschütz, F., Amor, J. M. and Wijmstra, T. A.: Palynology of a thick quaternary succession in
841 southern Spain, *Palaeogeogr. Palaeoclimatol. Palaeoecol.*, 10(4), 233–264,
842 doi:[http://dx.doi.org/10.1016/0031-0182\(71\)90049-6](http://dx.doi.org/10.1016/0031-0182(71)90049-6), 1971.

843 García-Alix, A., Jimenez-Espejo, F. J., Lozano, J. A., Jiménez-Moreno, G., Martínez-Ruiz, F.,
844 Sanjuán, L. G., Jiménez, G. A., Alfonso, E. G., Ruiz-Puertas, G. and Anderson, R. S.:
845 Anthropogenic impact and lead pollution throughout the Holocene in Southern Iberia, *Sci. Total*
846 *Environ.*, 449, 451–460, doi:<https://doi.org/10.1016/j.scitotenv.2013.01.081>, 2013.

847 García-Alix, A., Jiménez-Espejo, F. J., Toney, J. L., Jiménez-Moreno, G., Ramos-Román, M. J.,
848 Anderson, R. S., Ruano, P., Queralt, I., Delgado Huertas, A. and Kuroda, J.: Alpine bogs of
849 southern Spain show human-induced environmental change superimposed on long-term
850 natural variations, *Sci. Rep.*, 7(1), 7439, doi:10.1038/s41598-017-07854-w, 2017.

851 van Geel, B., Hallewas, D. P. and Pals, J. P.: A late holocene deposit under the Westfriese Zeedijk
852 near Enkhuizen (Prov. of Noord-Holland, The Netherlands): Palaeoecological and archaeological
853 aspects, *Rev. Palaeobot. Palynol.*, 38(3), 269–335, doi:[http://dx.doi.org/10.1016/0034-](http://dx.doi.org/10.1016/0034-6667(83)90026-X)
854 [6667\(83\)90026-X](http://dx.doi.org/10.1016/0034-6667(83)90026-X), 1983.

855 van Geel, B., Coope, G. R. and Hammen, T. V. D.: Palaeoecology and stratigraphy of the
856 lateglacial type section at Usselo (the Netherlands), *Rev. Palaeobot. Palynol.*, 60(1), 25–129,
857 doi:[http://dx.doi.org/10.1016/0034-6667\(89\)90072-9](http://dx.doi.org/10.1016/0034-6667(89)90072-9), 1989.

858 Gil García, M. J., Ruiz Zapata, M. B., Santisteban, J. I., Mediavilla, R., López-Pamo, E. and Dabrio,
859 C. J.: Late holocene environments in Las Tablas de Daimiel (south central Iberian peninsula,
860 Spain), *Veg. Hist. Archaeobotany*, 16(4), 241–250, doi:10.1007/s00334-006-0047-9, 2007.

861 Gil-Romera, G., Carrión, J. S., Pausas, J. G., Sevilla-Callejo, M., Lamb, H. F., Fernández, S. and
862 Burjachs, F.: Holocene fire activity and vegetation response in South-Eastern Iberia, *Quat. Sci.*
863 *Rev.*, 29(9), 1082–1092, doi:10.1016/j.quascirev.2010.01.006, 2010.

864 Grimm, E. C.: CONISS: a FORTRAN 77 program for stratigraphically constrained cluster analysis
865 by the method of incremental sum of squares, *Comput. Geosci.*, 13(1), 13–35,
866 doi:[http://dx.doi.org/10.1016/0098-3004\(87\)90022-7](http://dx.doi.org/10.1016/0098-3004(87)90022-7), 1987.

867 Guy-Ohlson, D.: Botryococcus as an aid in the interpretation of palaeoenvironment and
868 depositional processes, *Rev. Palaeobot. Palynol.*, 71(1), 1–15,
869 doi:[http://dx.doi.org/10.1016/0034-6667\(92\)90155-A](http://dx.doi.org/10.1016/0034-6667(92)90155-A), 1992.

870 Hurrell, J. W.: Decadal Trends in the North Atlantic Oscillation: Regional Temperatures and
871 Precipitation, *Science*, 269(5224), 676, doi:10.1126/science.269.5224.676, 1995.

872 Jalut, G., Dedoubat, J. J., Fontugne, M. and Otto, T.: Holocene circum-Mediterranean vegetation
873 changes: Climate forcing and human impact, *Quat. Int.*, 200(1–2), 4–18,
874 doi:<https://doi.org/10.1016/j.quaint.2008.03.012>, 2009.

875 Jiménez-Espejo, F. J., García-Alix, A., Jiménez-Moreno, G., Rodrigo-Gámiz, M., Anderson, R. S.,
876 Rodríguez-Tovar, F. J., Martínez-Ruiz, F., Giralt, S., Delgado Huertas, A. and Pardo-Igúzquiza, E.:
877 Saharan aeolian input and effective humidity variations over western Europe during the
878 Holocene from a high altitude record, *Chem. Geol.*, 374–375, 1–12,
879 doi:10.1016/j.chemgeo.2014.03.001, 2014.

880 Jiménez-Moreno, G. and Anderson, R. S.: Holocene vegetation and climate change recorded in
881 alpine bog sediments from the Borreguiles de la Virgen, Sierra Nevada, southern Spain, *Quat.*
882 *Res.*, 77(1), 44–53, doi:10.1016/j.yqres.2011.09.006, 2012.

883 Jiménez-Moreno, G., García-Alix, A., Hernández-Corbalán, M. D., Anderson, R. S. and Delgado-
884 Huertas, A.: Vegetation, fire, climate and human disturbance history in the southwestern
885 Mediterranean area during the late Holocene, *Quat. Res.*, 79(2), 110–122,
886 doi:https://doi.org/10.1016/j.yqres.2012.11.008, 2013.

887 Jiménez-Moreno, G., Rodríguez-Ramírez, A., Pérez-Asensio, J. N., Carrión, J. S., López-Sáez, J. A.,
888 Villarías-Robles, J. J. R., Celestino-Pérez, S., Cerrillo-Cuenca, E., León, Á. and Contreras, C.:
889 Impact of late-Holocene aridification trend, climate variability and geodynamic control on the
890 environment from a coastal area in SW Spain, *Holocene*, 25(4), 607–617,
891 doi:10.1177/0959683614565955, 2015.

892 Kalugin, I., Daryin, A., Smolyaninova, L., Andreev, A., Diekmann, B. and Khlystov, O.: 800-yr-long
893 records of annual air temperature and precipitation over southern Siberia inferred from
894 Teletskoye Lake sediments, *Quat. Res.*, 67(3), 400–410,
895 doi:https://doi.org/10.1016/j.yqres.2007.01.007, 2007.

896 Laskar, J., Robutel, P., Joutel, F., Gastineau, M., Correia, A. C. M. and Levrard, B.: A long-term
897 numerical solution for the insolation quantities of the Earth, *A&A*, 428(1), 261–285,
898 doi:10.1051/0004-6361:20041335, 2004.

899 Lebreiro, S. M., Francés, G., Abrantes, F. F. G., Diz, P., Bartels-Jónsdóttir, H. B., Stroynowski, Z.
900 N., Gil, I. M., Pena, L. D., Rodrigues, T., Jones, P. D., Nombela, M. A., Alejo, I., Briffa, K. R., Harris,
901 I. and Grimalt, J. O.: Climate change and coastal hydrographic response along the Atlantic
902 Iberian margin (Tagus Prodelta and Muros Ría) during the last two millennia, *Holocene*, 16(7),
903 1003–1015, doi:10.1177/0959683606h1990rp, 2006.

904 Lillios, K. T., Blanco-González, A., Drake, B. L. and López-Sáez, J. A.: Mid-late Holocene climate,
905 demography, and cultural dynamics in Iberia: A multi-proxy approach, *Quat. Sci. Rev.*, 135, 138–
906 153, doi:https://doi.org/10.1016/j.quascirev.2016.01.011, 2016.

907 López-Sáez, J. A., Abel-Schaad, D., Pérez-Díaz, S., Blanco-González, A., Alba-Sánchez, F., Dorado,
908 M., Ruiz-Zapata, B., Gil-García, M. J., Gómez-González, C. and Franco-Múgica, F.: Vegetation
909 history, climate and human impact in the Spanish Central System over the last 9000 years,
910 *Quat. Int.*, 353, 98–122, doi:https://doi.org/10.1016/j.quaint.2013.06.034, 2014.

- 911 Lukianova, R. and Alekseev, G.: Long-Term Correlation Between the Nao and Solar Activity, *Sol.*
912 *Phys.*, 224(1), 445–454, doi:10.1007/s11207-005-4974-x, 2004.
- 913 Magny, M.: Holocene climate variability as reflected by mid-European lake-level fluctuations
914 and its probable impact on prehistoric human settlements, *Quat. Int.*, 113(1), 65–79,
915 doi:https://doi.org/10.1016/S1040-6182(03)00080-6, 2004.
- 916 Magny, M., Peyron, O., Sadori, L., Ortu, E., Zanchetta, G., Vannièrè, B. and Tinner, W.:
917 Contrasting patterns of precipitation seasonality during the Holocene in the south- and north-
918 central Mediterranean, *J. Quat. Sci.*, 27(3), 290–296, doi:10.1002/jqs.1543, 2012.
- 919 Magri, D.: Late Quaternary vegetation history at Lagaccione near Lago di Bolsena (central Italy),
920 *Rev. Palaeobot. Palynol.*, 106(3–4), 171–208, doi:https://doi.org/10.1016/S0034-
921 6667(99)00006-8, 1999.
- 922 Marchal, O., Cacho, I., Stocker, T. F., Grimalt, J. O., Calvo, E., Martrat, B., Shackleton, N.,
923 Vautravers, M., Cortijo, E., Van Kreveld, S., Andersson, C., Koç, N., Chapman, M., Sbaffi, L.,
924 Duplessy, J.-C., Sarnthein, M., Turon, J.-L., Duprat, J. and Jansen, E.: Apparent long-term cooling
925 of the sea surface in the northeast Atlantic and Mediterranean during the Holocene, *Quat. Sci.*
926 *Rev.*, 21(4–6), 455–483, doi:10.1016/S0277-3791(01)00105-6, 2002.
- 927 Martín-Puertas, C., Valero-Garcés, B. L., Mata, M. P., González-Sampériz, P., Bao, R., Moreno, A.
928 and Stefanova, V.: Arid and humid phases in southern Spain during the last 4000 years: the
929 Zoñar Lake record, Córdoba, *The Holocene*, 18(6), 907–921, doi:10.1177/0959683608093533,
930 2008.
- 931 Martín-Puertas, C., Valero-Garcés, B. L., Brauer, A., Mata, M. P., Delgado-Huertas, A. and Dulski,
932 P.: The Iberian-Roman Humid Period (2600-1600 cal yr BP) in the Zoñar Lake varve record
933 (Andalucía, southern Spain), *Quat. Res.*, 71(2), 108–120, doi:10.1016/j.yqres.2008.10.004, 2009.
- 934 Martín-Puertas, C., Valero-Garcés, B. L., Mata, M. P., Moreno, A., Giral, S., Martínez-Ruiz, F.
935 and Jiménez-Espejo, F.: Geochemical processes in a Mediterranean Lake: A high-resolution
936 study of the last 4,000 years in Zoñar Lake, southern Spain, *J. Paleolimnol.*, 46(3), 405–421,
937 doi:10.1007/s10933-009-9373-0, 2011.
- 938 Mayewski, P. A., Rohling, E. E., Stager, J. C., Karlén, W., Maasch, K. A., Meeker, L. D., Meyerson,
939 E. A., Gasse, F., Kreveld, S. van, Holmgren, K., Lee-Thorp, J., Rosqvist, G., Rack, F., Staubwasser,
940 M., Schneider, R. R. and Steig, E. J.: Holocene climate variability, *Quat. Res.*, 62(3), 243–255,
941 doi:https://doi.org/10.1016/j.yqres.2004.07.001, 2004.
- 942 Mercuri, A. M., Accorsi, C. A., Mazzanti, M. B., Bosi, G., Cardarelli, A., Labate, D., Marchesini, M.
943 and Grandi, G. T.: Economy and environment of Bronze Age settlements – Terramaras – on the
944 Po Plain (Northern Italy): first results from the archaeobotanical research at the Terramara di
945 Montale, *Veg. Hist. Archaeobotany*, 16(1), 43, doi:10.1007/s00334-006-0034-1, 2006.

946 Morellón, M., Valero-Garcés, B., Vegas-Vilarrúbia, T., González-Sampérez, P., Romero, Ó.,
947 Delgado-Huertas, A., Mata, P., Moreno, A., Rico, M. and Corella, J. P.: Lateglacial and Holocene
948 palaeohydrology in the western Mediterranean region: The Lake Estanya record (NE Spain),
949 *Quat. Sci. Rev.*, 28(25–26), 2582–2599, doi:<https://doi.org/10.1016/j.quascirev.2009.05.014>,
950 2009.

951 Morellón, M., Valero-Garcés, B., González-Sampérez, P., Vegas-Vilarrúbia, T., Rubio, E.,
952 Rieradevall, M., Delgado-Huertas, A., Mata, P., Romero, Ó., Engstrom, D. R., López-Vicente, M.,
953 Navas, A. and Soto, J.: Climate changes and human activities recorded in the sediments of Lake
954 Estanya (NE Spain) during the Medieval Warm Period and Little Ice Age, *J. Paleolimnol.*, 46(3),
955 423–452, doi:10.1007/s10933-009-9346-3, 2011.

956 Morellón, M., Anselmetti, F. S., Ariztegui, D., Brushulli, B., Sinopoli, G., Wagner, B., Sadori, L.,
957 Gilli, A. and Pambuku, A.: Human–climate interactions in the central Mediterranean region
958 during the last millennia: The laminated record of Lake Butrint (Albania), *Spec. Issue Mediterr.*
959 *Holocene Clim. Environ. Hum. Soc.*, 136(Supplement C), 134–152,
960 doi:10.1016/j.quascirev.2015.10.043, 2016.

961 Moreno, A., Cacho, I., Canals, M., Grimalt, J. O., Sánchez-Goñi, M. F., Shackleton, N. and Sierro,
962 F. J.: Links between marine and atmospheric processes oscillating on a millennial time-scale. A
963 multi-proxy study of the last 50,000 yr from the Alboran Sea (Western Mediterranean Sea),
964 *Quat. Sci. Rev.*, 24(14–15), 1623–1636, doi:<https://doi.org/10.1016/j.quascirev.2004.06.018>,
965 2005.

966 Moreno, A., Pérez, A., Frigola, J., Nieto-Moreno, V., Rodrigo-Gámiz, M., Martrat, B., González-
967 Sampérez, P., Morellón, M., Martín-Puertas, C., Corella, J. P., Belmonte, Á., Sancho, C., Cacho, I.,
968 Herrera, G., Canals, M., Grimalt, J. O., Jiménez-Espejo, F., Martínez-Ruiz, F., Vegas-Vilarrúbia, T.
969 and Valero-Garcés, B. L.: The Medieval Climate Anomaly in the Iberian Peninsula reconstructed
970 from marine and lake records, *Quat. Sci. Rev.*, 43, 16–32,
971 doi:<https://doi.org/10.1016/j.quascirev.2012.04.007>, 2012.

972 Nestares, T. and Torres, T. de: Un nuevo sondeo de investigación paleoambiental del
973 Pleistoceno y Holoceno en la turbera del Padul (Granada, Andalucía). *Geogaceta* 23, 99-102.,
974 1997.

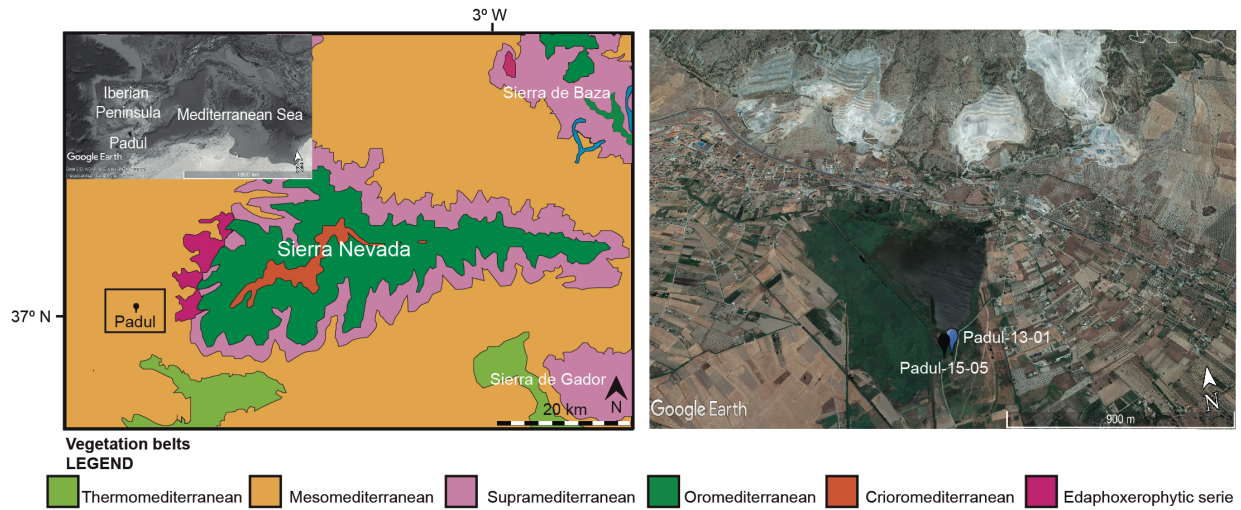
975 Olsen, J., Anderson, N. J. and Knudsen, M. F.: Variability of the North Atlantic Oscillation over
976 the past 5,200 years, *Nat. Geosci*, 5(11), 808–812, doi:10.1038/ngeo1589, 2012.

977 Ortiz, J. E., Torres, T., Delgado, A., Julià, R., Lucini, M., Llamas, F. J., Reyes, E., Soler, V. and Valle,
978 M.: The palaeoenvironmental and palaeohydrological evolution of Padul Peat Bog (Granada,
979 Spain) over one million years, from elemental, isotopic and molecular organic geochemical
980 proxies, *Org. Geochem.*, 35(11–12), 1243–1260,
981 doi:<https://doi.org/10.1016/j.orggeochem.2004.05.013>, 2004.

- 982 Paillard, D., Labeyrie, L. and Yiou, P.: Macintosh Program performs time-series analysis, *Eos*
983 *Trans. Am. Geophys. Union*, 77(39), 379–379, doi:10.1029/96EO00259, 1996.
- 984 Pérez Raya, F. and López Nieto, J.: Vegetación acuática y helofítica de la depresión de Padul
985 (Granada), *Acta Bot Malacit.*, 16(2), 373–389, 1991.
- 986 Pons, A. and Reille, M.: The holocene- and upper pleistocene pollen record from Padul
987 (Granada, Spain): A new study, *Palaeogeogr. Palaeoclimatol. Palaeoecol.*, 66(3), 243–263,
988 doi:http://dx.doi.org/10.1016/0031-0182(88)90202-7, 1988.
- 989 Ramos-Román, M. J., Jiménez-Moreno, G., Anderson, R. S., García-Alix, A., Toney, J. L., Jiménez-
990 Espejo, F. J. and Carrión, J. S.: Centennial-scale vegetation and North Atlantic Oscillation
991 changes during the Late Holocene in the southern Iberia, *Quat. Sci. Rev.*, 143, 84–95,
992 doi:https://doi.org/10.1016/j.quascirev.2016.05.007, 2016.
- 993 Reimer, P. J., Bard, E., Bayliss, A., Beck, J. W., Blackwell, P. G., Ramsey, C. B., Buck, C. E., Cheng,
994 H., Edwards, R. L., Friedrich, M., Grootes, P. M., Guilderson, T. P., Haflidason, H., Hajdas, I.,
995 Hatté, C., Heaton, T. J., Hoffmann, D. L., Hogg, A. G., Hughen, K. A., Kaiser, K. F., Kromer, B.,
996 Manning, S. W., Niu, M., Reimer, R. W., Richards, D. A., Scott, E. M., Southon, J. R., Staff, R. A.,
997 Turney, C. S. M. and van der Plicht, J.: IntCal13 and Marine13 Radiocarbon Age Calibration
998 Curves 0–50,000 Years cal BP, *Radiocarbon*, 55(4), 1869–1887, doi:10.2458/azu_js_rc.55.16947,
999 2013.
- 1000 Riera, S., Wansard, G. and Julià, R.: 2000-year environmental history of a karstic lake in the
1001 Mediterranean Pre-Pyrenees: the Estanya lakes (Spain), *{CATENA}*, 55(3), 293–324,
1002 doi:https://doi.org/10.1016/S0341-8162(03)00107-3, 2004.
- 1003 Riera, S., López-Sáez, J. A. and Julià, R.: Lake responses to historical land use changes in
1004 northern Spain: The contribution of non-pollen palynomorphs in a multiproxy study, *Rev.*
1005 *Palaeobot. Palynol.*, 141(1–2), 127–137, doi:https://doi.org/10.1016/j.revpalbo.2006.03.014,
1006 2006.
- 1007 Roberts, N., Brayshaw, D., Kuzucuoğlu, C., Perez, R. and Sadori, L.: The mid-Holocene climatic
1008 transition in the Mediterranean: Causes and consequences, *The Holocene*, 21(1), 3–13,
1009 doi:10.1177/0959683610388058, 2011.
- 1010 Rodrigo-Gámiz, M., Martínez-Ruiz, F., Rodríguez-Tovar, F. J., Jiménez-Espejo, F. J. and Pardo-
1011 Igúzquiza, E.: Millennial- to centennial-scale climate periodicities and forcing mechanisms in the
1012 westernmost Mediterranean for the past 20,000 yr, *Quat. Res.*, 81(1), 78–93,
1013 doi:https://doi.org/10.1016/j.yqres.2013.10.009, 2014.
- 1014 Sadori, L., Jahns, S. and Peyron, O.: Mid-Holocene vegetation history of the central
1015 Mediterranean, *The Holocene*, 21(1), 117–129, doi:10.1177/0959683610377530, 2011.
- 1016 Sadori, L., Giraudi, C., Masi, A., Magny, M., Ortu, E., Zanchetta, G. and Izdebski, A.: Climate,
1017 environment and society in southern Italy during the last 2000 years. A review of the

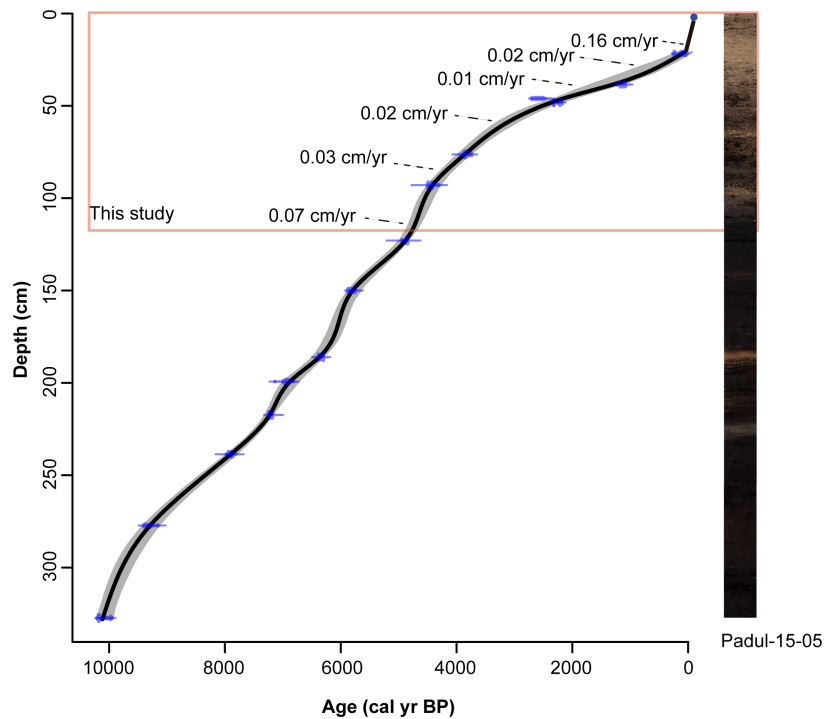
- 1018 environmental, historical and archaeological evidence, Spec. Issue Mediterr. Holocene Clim.
1019 Environ. Hum. Soc., 136(Supplement C), 173–188, doi:10.1016/j.quascirev.2015.09.020, 2016.
- 1020 Sanz de Galdeano, C., El Hamdouni, R. and Chacón, J.: Neotectónica de la fosa del Padul y del
1021 Valle de Lecrín, Itiner. Geomorfológicos Por Andal. Orient. Publicacions Univ. Barc. Barc., 65–81,
1022 1998.
- 1023 Sicre, M.-A., Jalali, B., Martrat, B., Schmidt, S., Bassetti, M.-A. and Kallel, N.: Sea surface
1024 temperature variability in the North Western Mediterranean Sea (Gulf of Lion) during the
1025 Common Era, Earth Planet. Sci. Lett., 456, 124–133,
1026 doi:http://dx.doi.org/10.1016/j.epsl.2016.09.032, 2016.
- 1027 Sonett, C. P. and Suess, H. E.: Correlation of bristlecone pine ring widths with atmospheric ¹⁴C
1028 variations: a climate-Sun relation, Nature, 307(5947), 141–143, doi:10.1038/307141a0, 1984.
- 1029 Steinhilber, F., Beer, J. and Fröhlich, C.: Total solar irradiance during the Holocene, Geophys.
1030 Res. Lett., 36(19), n/a–n/a, doi:10.1029/2009GL040142, 2009.
- 1031 Trouet, V., Esper, J., Graham, N. E., Baker, A., Scourse, J. D. and Frank, D. C.: Persistent Positive
1032 North Atlantic Oscillation Mode Dominated the Medieval Climate Anomaly, Science, 324(5923),
1033 78, doi:10.1126/science.1166349, 2009.
- 1034 Villegas Molina, F.: Laguna de Padul: Evolución geológico-histórica, Estud. Geográficos, 28(109),
1035 561, 1967.
- 1036 Zanchettin, D., Rubino, A., Traverso, P. and Tomasino, M.: Impact of variations in solar activity
1037 on hydrological decadal patterns in northern Italy, J. Geophys. Res. Atmospheres, 113(D12),
1038 n/a–n/a, doi:10.1029/2007JD009157, 2008.

1039 **Figures and tables**



1040

1041 **Figure 1.** Location of Padul peat bog in Sierra Nevada, southern Iberian Peninsula. Panel on the
1042 left is the map of the vegetation belts in the Sierra Nevada (Modified from REDIAM. Map of the
1043 vegetation series of Andalucía:
1044 [http://laboratoriolediam.cica.es/VisorGenerico/?tipo=WMS&url=http://www.juntadeandalucia.e](http://laboratoriolediam.cica.es/VisorGenerico/?tipo=WMS&url=http://www.juntadeandalucia.es/medioambiente/mapwms/REDIAM_Series_Vegetacion_Andalucia?)
1045 [s/medioambiente/mapwms/REDIAM_Series_Vegetacion_Andalucia?](http://www.juntadeandalucia.es/medioambiente/mapwms/REDIAM_Series_Vegetacion_Andalucia?)). The inset map is the
1046 Google earth image of the Iberian Peninsula in the Mediterranean region. Panel on the right is
1047 the Google earth image (<http://www.google.com/earth/index.html>) of Padul peat bog area
1048 showing the coring locations.

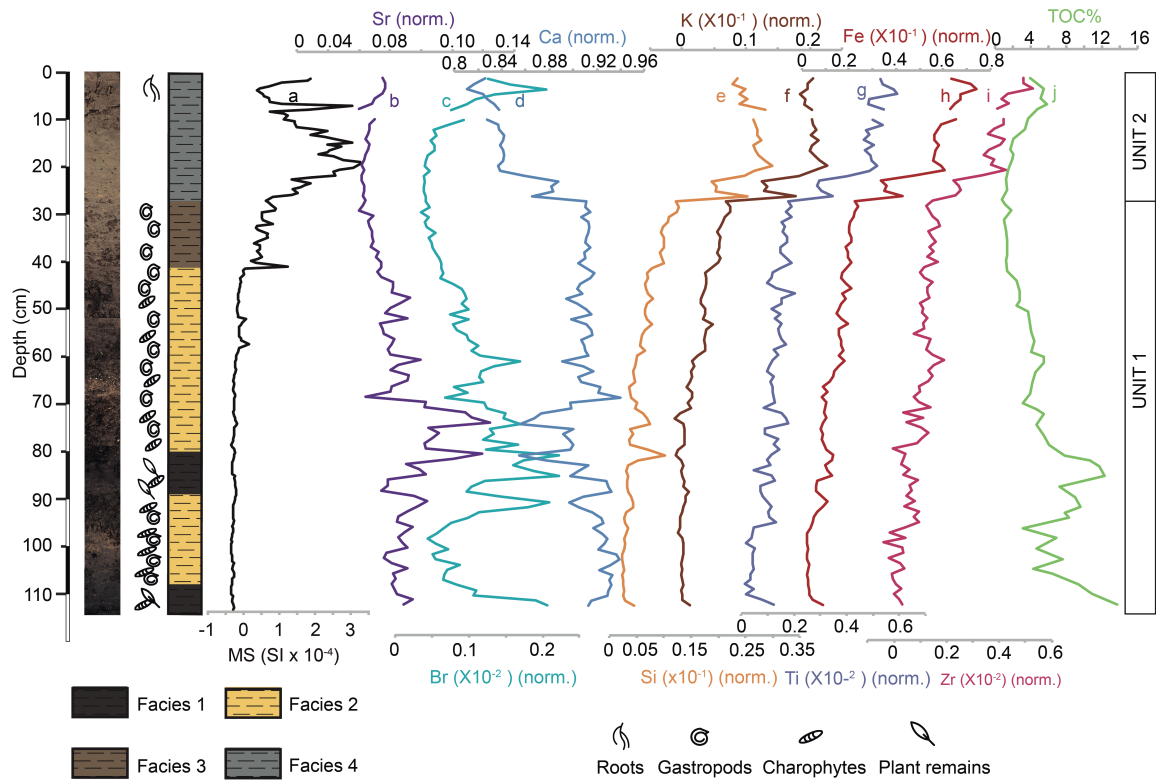


1049

1050 **Figure 2.** Photo of the Padul-15-05 sediment core with the age-depth model showing the part of
 1051 the record that was studied here (red rectangle). The sediment accumulation rates (SAR) between
 1052 individual segments are marked. See the body of the text for the explanation of the age
 1053 reconstructions.

1054

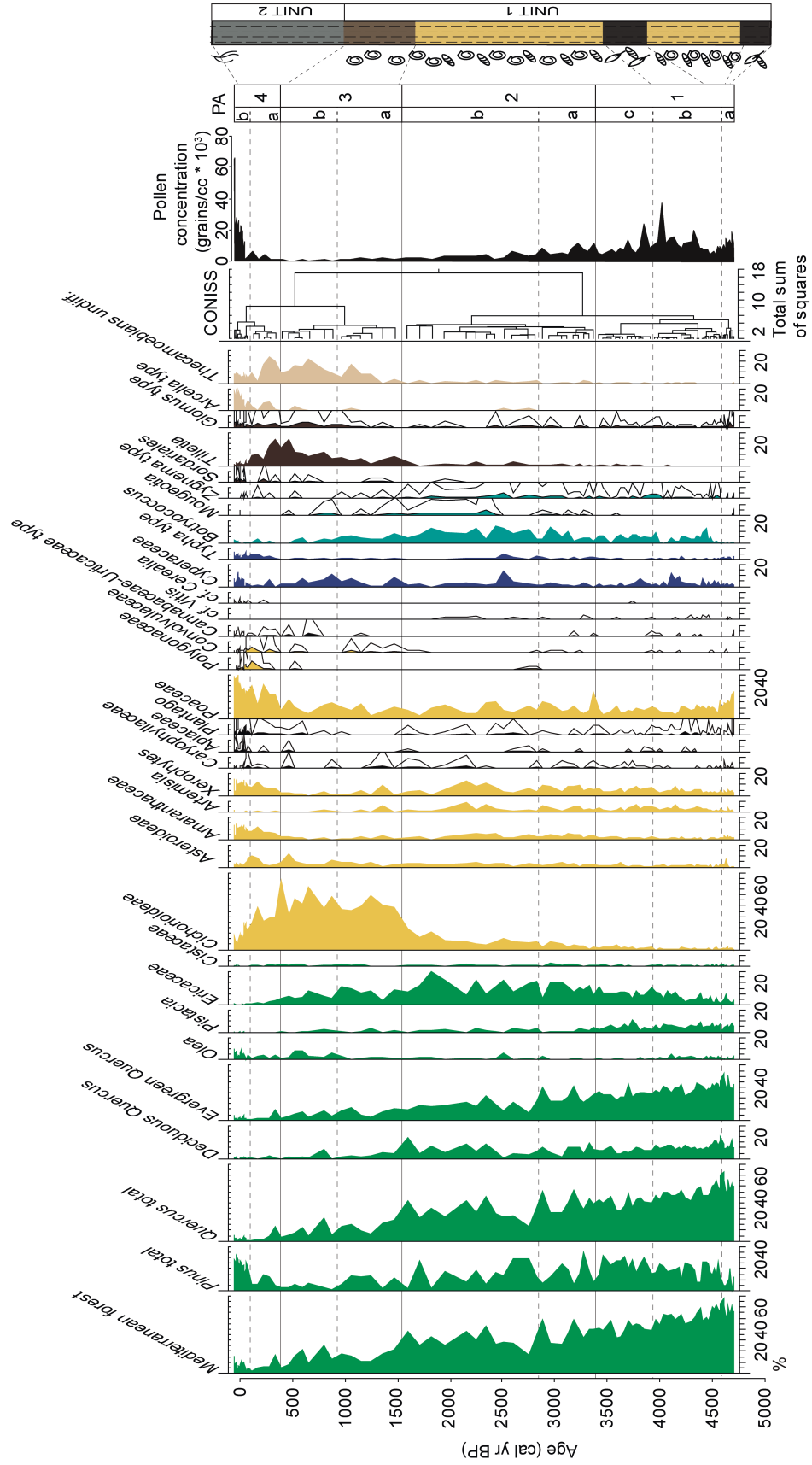
1055



1056

1057 **Figure 3.** Lithology, facies interpretation with paleontology, magnetic susceptibility (MS), and
 1058 geochemical (X-ray fluorescence (XRF) and total organic carbon (TOC) data from the Padul-15-
 1059 05 record. XRF elements are represented normalized by the total counts. (a) Magnetic
 1060 susceptibility (MS; SI units). (b) Strontium normalized (Sr; norm.). (c) Bromine norm. (Br;
 1061 norm.). (d) Calcium normalized. (Ca; norm.). (e) Silica normalized (Si; norm.). (f) Potassium
 1062 normalized (K; norm.). (g) Titanium normalized (Ti; norm.). (h) Iron normalized (Fe; norm.). (i)
 1063 Zirconium normalized (Zr; norm.). (j) Total organic carbon (TOC %).

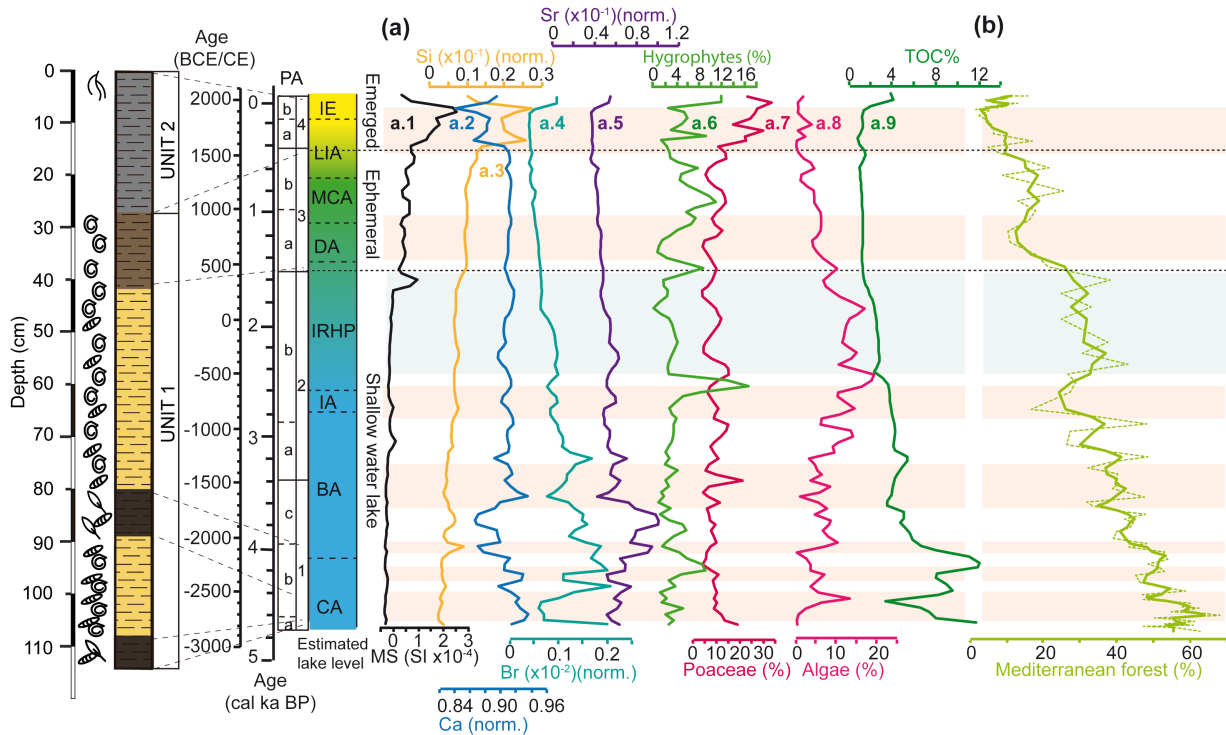
1064



1066

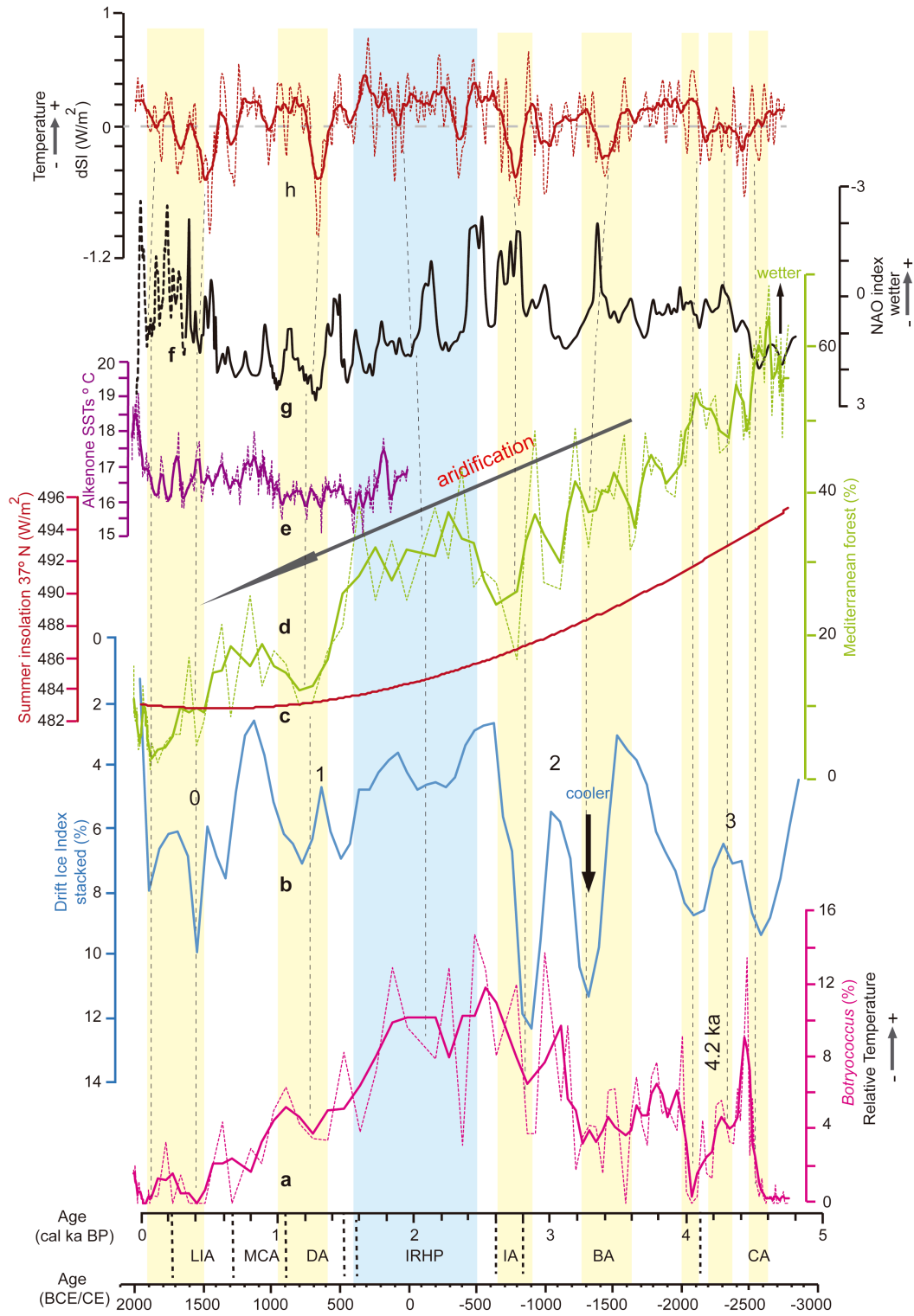
1067 **Figure 4.** Percentages of selected pollen taxa and non-pollen palynomorphs (NPPs) from the
1068 Padul-15-05 record, calculated with respect to terrestrial pollen sum. Silhouettes show 7-time
1069 exaggerations of pollen percentages. Pollen zonation, pollen concentration (grains/cc) and
1070 lithology are shown on the right. Tree and shrubs are showing in green, herbs and grasses in
1071 yellow, aquatics in dark blue, algae in blue, fungi in brown and thecamoebians in beige. The
1072 Mediterranean forest taxa category is composed of *Quercus* total, *Olea*, *Phillyrea* and *Pistacia*.
1073 The xerophyte group includes *Artemisia*, *Ephedra*, and Amaranthaceae. PA = Pollen zones.

1074



1075

1076 **Figure 5.** Estimated lake level evolution and regional palynological component from the last ca.
 1077 4700 yr based on the synthesis of determinate proxies from the Padul-15-05 record: (a) Proxies
 1078 used to estimate the water table evolution from the Padul-15-05 record (proxies were resampled
 1079 at 50 yr (lineal interpolation) using Past software [http://palaeo-](http://palaeo-electronica.org/2001_1/past/issue1_01.htm)
 1080 [electronica.org/2001_1/past/issue1_01.htm](http://palaeo-electronica.org/2001_1/past/issue1_01.htm)). [(a.1) Magnetic Susceptibility (MS) in SI; (a.2)
 1081 Silica normalized (Si; norm.); (a.3) Calcium normalized (Ca; norm.); (a.4) Bromine normalized
 1082 (Br; norm.); (a.5) Strontium normalized (Sr; norm.); (a.6) Hygrophytes (%); (a.7) Poaceae (%);
 1083 (a.8) Algae (%) (a.9) Total organic carbon (TOC %)] (b) Mediterranean forest taxa, with a
 1084 smoothing of three-point in bold. Pink and blue shading indicates Holocene arid and humid
 1085 regionally events, respectively. See the body of the text for the explanation of the lake level
 1086 reconstruction. Mediterranean forest smoothing was made using Analyseries software (Paillard
 1087 et al., 1996). PA = Pollen Zones; CA = Copper Age; BA = Bronze Age; IA = Iron Age; IRHP =
 1088 Iberian Roman Humid Period; DA = Dark Ages; MCA = Medieval Climate Anomaly; LIA =
 1089 Little Ice Age; IE = Industrial Era.



1090

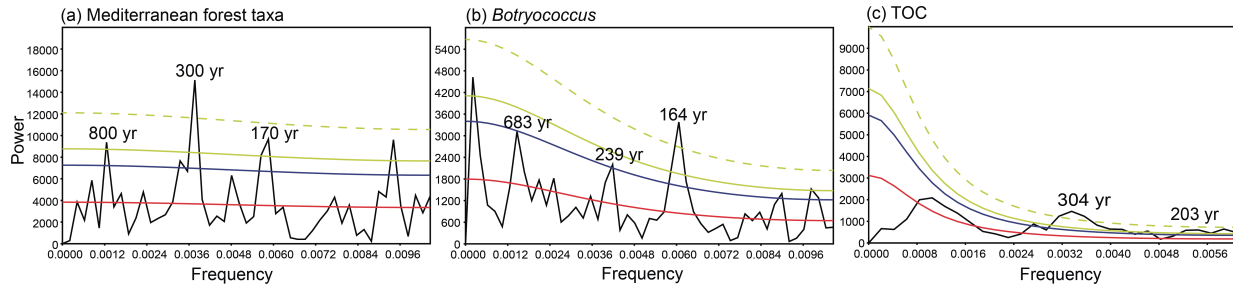
1091

1092

1093 **Figure 6.** Comparison of the last ca. 4700 yr between different pollen taxa from the Padul-15-05
1094 record, summer insolation for the Sierra Nevada latitude, eastern Mediterranean humidity and
1095 North Atlantic temperature. (a) *Botryococcus* from the Padul-15-05 record, with a smoothing of
1096 three-point in bold (this study). (b) Drift Ice Index (reversed) from the North Atlantic (Bond et
1097 al., 2001). (c) Summer insolation calculated for 37° N (Laskar et al., 2004). (d) Mediterranean
1098 forest taxa from the Padul-15-05 record, with a smoothing of three-point in bold (this study). (e)
1099 Alkenone-SSTs from the Gulf of Lion (Sicre et al., 2016), with a smoothing of four-point in
1100 bold. (f) North Atlantic Oscillation (NAO) index from a climate proxy reconstruction from
1101 Morocco and Scotland (Trouet et al., 2009). (g) North Atlantic Oscillation (NAO) index
1102 (reversed) from a climate proxy reconstruction from Greenland (Olsen et al., 2012). (h) Total
1103 solar irradiance reconstruction from cosmogenic radionuclide from a Greenland ice core
1104 (Steinhilber et al., 2009), with a smoothing of twenty-one-point in bold. Yellow and blue shading
1105 correspond with arid (and cold) and humid (and warm) periods, respectively. Grey dash lines
1106 show a tentative correlation between arid and cold conditions and the decrease in the
1107 Mediterranean forest and *Botryococcus*. Mediterranean forest, *Botryococcus* and solar irradiance
1108 smoothing was made using Analyseries software (Paillard et al., 1996), Alkenone-SSTs
1109 smoothing was made using Past software ([http://palaeo-](http://palaeo-electronica.org/2001_1/past/issue1_01.htm)
1110 [electronica.org/2001_1/past/issue1_01.htm](http://palaeo-electronica.org/2001_1/past/issue1_01.htm)). A linear r (Pearson) correlation was calculated
1111 between *Botryococcus* (detrended) and Drift Ice Index (Bond et al., 2001; $r = -0.63$; $p < 0.0001$;
1112 between ca. 4700 to 1500 cal ka BP – $r = -0.48$; $p < 0.0001$ between 4700 and -65 cal yr BP).
1113 Previously, the data were detrended (only in *Botryococcus*), resampled at 70-yr (linear
1114 interpolation) in order to obtain equally spaced time series and smoothed to three-point average.
1115 CA = Copper Age; BA = Bronze Age; IA = Iron Age; IRHP = Iberian Roman Humid Period;
1116 DA = Dark Ages; MCA = Medieval Climate Anomaly; LIA = Little Ice Age; IE = Industrial Era.

1117

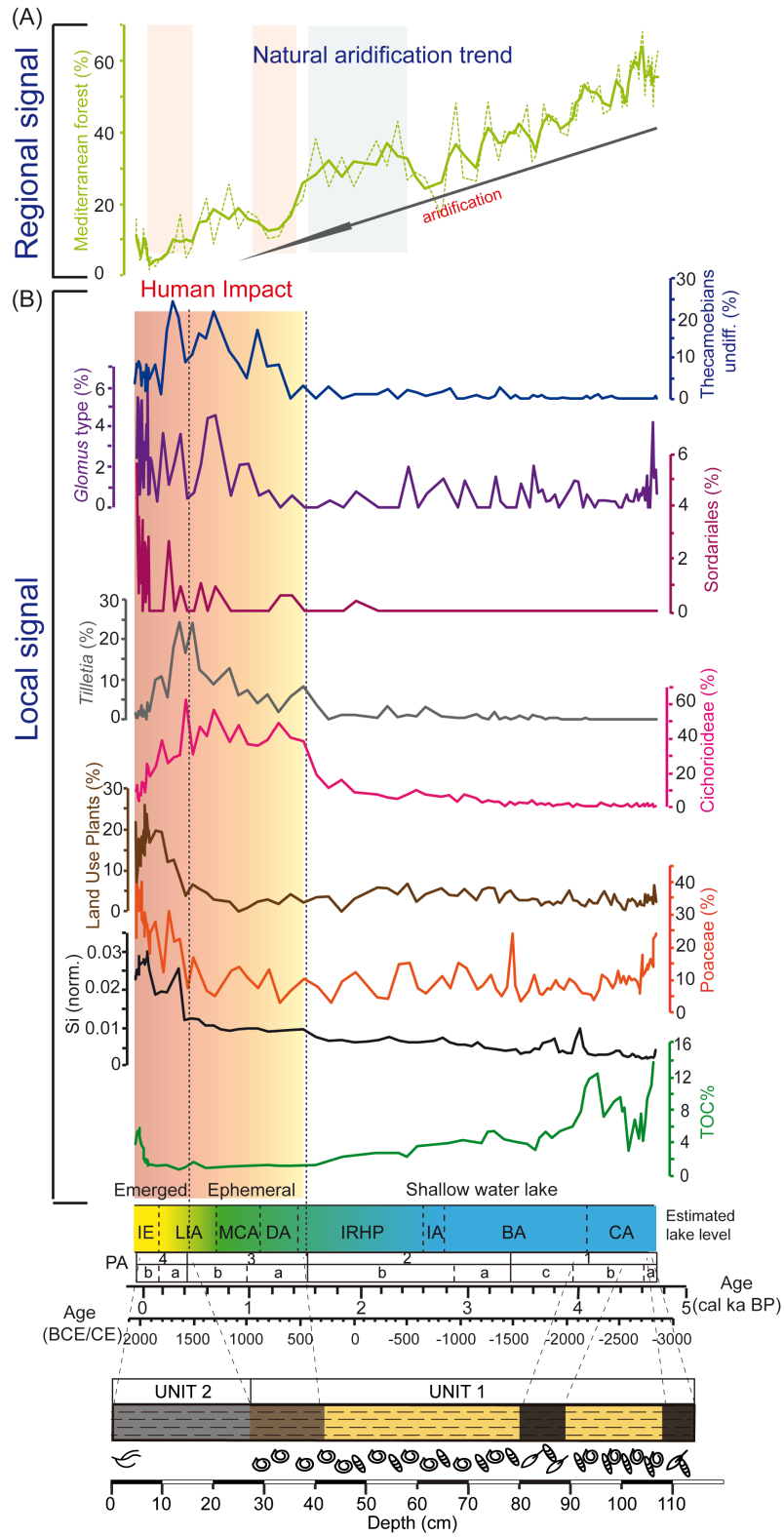
1118



1119

1120 **Figure 7.** Spectral analysis of (a) Mediterranean forest taxa and (b) *Botryococcus* (mean
 1121 sampling space = 47 yr) and (c) TOC (mean sampling space = 78 yr) from the Padul-15-05. The
 1122 significant periodicities above confident level are shown. Confidence level 90 % (blue line), 95
 1123 % (green line), 99 % (green dash line) and AR (1) red noise (red line). Spectral analysis was
 1124 made with Past software ([http://palaeo-
 electronica.org/2001_1/past/issue1_01.htm](http://palaeo-electronica.org/2001_1/past/issue1_01.htm)).

1125



1126

1127

1128

1129 **Figure 8.** Comparison of the last ca. 4700 yr between regional climatic proxies and local human
1130 activity indicators from the Padul-15-05 record. (a) Mediterranean forest taxa, with a smoothing
1131 of three-point in bold. (b) Local human activities indicators [(b.1) Total organic carbon (TOC
1132 %), soil erosion indicator; (b.2) Si normalized (Si, norm.), soil erosion indicator; (b.3) Poaceae
1133 (%), lake drained and/or cultivars indicator; (b.4) Land Use Plants (%), cultivar indicator; (b.5)
1134 Cichorioideae (%), livestock occurrence indicator; (b.6) *Tilletia* (%), farming indicator; (b.7)
1135 Sordariales (%), livestock indicator; (b.8) Thecamoebians undiff. (%), livestock indicator].
1136 Degraded yellow to red shading correspond with the time when we have evidence of human
1137 shaping the environment since ca. 1550 cal yr BP to Present. Previously to that period there is a
1138 lack of clear evidences of human impact in the area. Land use plants is composed by
1139 Polygonaceae, Amaranthaceae, Convolvulaceae, *Plantago*, Apiaceae and Cannabaceae-
1140 Urticaceae type.

1141 **Table 1.** Age data for Padul-15-05 record. All ages were calibrated using R-code package ‘clam
 1142 2.2’ employing the calibration curve IntelCal 13 (Reimer et al., 2013) at 95 % of confident range.

1143 *Sample number assigned at radiocarbon laboratory

Laboratory number	Core	Material	Depth (cm)	Age (¹⁴ C yr BP ± 1σ)	Calibrated age (cal yr BP) 95 % confidence interval	Median age (cal yr BP)
Reference ages			0	2015CE	-65	-65
D-AMS 008531	Padul-13-01	Plant remains	21.67	103 ± 24	23-264	127
Poz-77568	Padul-15-05	Org. bulk sed.	38.46	1205 ± 30	1014-1239	1130
BETA-437233	Padul-15-05	Plant remains	46.04	2480 ± 30	2385-2722	2577
Poz-77569	Padul-15-05	Org. bulk sed.	48.21	2255 ± 30	2158-2344	2251
BETA-415830	Padul-15-05	Shell	71.36	3910 ± 30	4248-4421	4343
BETA-437234	Padul-15-05	Plant remains	76.34	3550 ± 30	3722-3956	3838
BETA-415831	Padul-15-05	Org. bulk sed.	92.94	3960 ± 30	4297-4519	4431
Poz-74344	Padul-15-05	Plant remains	122.96	4295 ± 35	4827-4959	4871
BETA-415832	Padul-15-05	Plant remains	150.04	5050 ± 30	5728-5900	5814
Poz-77571	Padul-15-05	Plant remains	186.08	5530 ± 40	6281-6402	6341
Poz-74345	Padul-15-05	Plant remains	199.33	6080 ± 40	6797-7154	6935
BETA-415833	Padul-15-05	Org. bulk sed.	217.36	6270 ± 30	7162-7262	7212
Poz-77572	Padul-15-05	Org. bulk sed.	238.68	7080 ± 50	7797-7999	7910
Poz-74347	Padul-15-05	Plant remains	277.24	8290 ± 40	9138-9426	9293
BETA-415834	Padul-15-05	Plant remains	327.29	8960 ± 30	9932-10221	10107

1144

1145

1146 **Table 2.** Linear r (Pearson) correlation between geochemical elements from the Padul-15-05
 1147 record. Statistical treatment was performed using the Past software ([http://palaeo-
 electronica.org/2001_1/past/issue1_01.htm](http://palaeo-

 1148 electronica.org/2001_1/past/issue1_01.htm)).

1149

	Si	K	Ca	Ti	Fe	Zr	Br	Sr
Si		8.30E-80	2.87E-34	7.47E-60	3.22E-60	5.29E-44	0.001152	7.79E-09
K	0.98612		7.07E-29	6.05E-60	8.20E-68	1.77E-51	0.00030317	5.38E-12
Ca	-0.88096	-0.84453		6.09E-42	5.81E-39	8.10E-34	0.35819	0.26613
Ti	0.96486	0.96501	-0.91794		1.74E-74	1.12E-57	0.074223	8.88E-07
Fe	0.96546	0.97577	-0.90527	0.98224		2.77E-66	0.051072	3.32E-08
Zr	0.92566	0.94789	-0.8783	0.96109	0.97398		0.054274	7.16E-08
Br	-0.31739	-0.3506	-0.091917	-0.17755	-0.19372	-0.19116		4.03E-18
Sr	-0.53347	-0.61629	0.11113	-0.46426	-0.51386	-0.50295	0.72852	

1150

1151

1152

1153

1154

1155

1156

1157

1158

1159

1160

1161

1162

1163

1164

1165